This is a preprint, the final version is subject to change, of the American Mineralogist (MSA)
Cite as Authors (Year) Title. American Mineralogist, in press.
(DOI will not work until issue is live.) DOI: http://dx.doi.org/10.2138/am-2016-5683

American Mineralogist Manuscript 5683 Revision 1

Ideal Wollastonite and the Structural Relationship between the Pyroxenoids and Pyroxenes

Richard M. Thompson[1*], Hexiong Yang[2], and Robert T. Downs[2]

[1]School of Information, University of Arizona, 1103 E. 2nd Street, Tucson, Arizona 85721, U.S.A.

[2]Department of Geosciences, University of Arizona, 1040 E. 4th Street, Tucson, Arizona 85721, U.S.A.

*Corresponding author: rmthomps@email.arizona.edu

Abstract

A hypothetical ideal wollastonite with regular octahedra and T3 tetrahedron is presented and used to compare and contrast the pyroxenes and pyroxenoids. While clinopyroxenes have close-packed arrangements of oxygen anions, several lines of evidence demonstrate that pyroxenoids do not. One such line is the number of tetrahedra in a single tetrahedral chain per octahedra in a single associated octahedral chain (interior to the octahedral band), referred to as the "single chain T:O ratio", which is 1:1 in pyroxenes but 3:2 in wollastonite and always greater than 1:1 in other $MSiO_3$ pyroxenoids. Because the Si-tetrahedron is extremely resistant to distortion, this forces marked distortion in at least one pyroxenoid octahedral site.

The octahedral layers in pyroxenes and pyroxenoids are compared by placing them in the context of a fully occupied, closest-packed sheet of idealized octahedra and it is shown that they are fundamentally different.

The new mineral yangite is analyzed from the perspective developed in this study. It is structurally similar to the pyroxenoids but the structure is a new type because it contains double tetrahedral chains and mixed polyhedral layers containing double chains of tetrahedra and bands of octahedra of width two. The tetrahedral chains are wollastonite-type chains and the wollastonite-type double chain is shown to have important differences from the amphibole

double chain. A possible explanation for the existence of this crystal structure based on a hydrogen bond between Pb and O is presented.

Key words: clinopyroxene, pyroxenoid, chain silicate, yangite, wollastonite, diopside, close-packing

Introduction

The new mineral yangite, a new type of chain silicate with double tetrahedral chains and ideal formula $PbMnSi_3O_8 \cdot H_2O$, is described elsewhere in this issue (Downs et al. this issue). This companion paper compares and contrasts the pyroxenoids and pyroxenes in order to develop some new approaches to characterizing and understanding members of the pyroxenoid group. To do so, this study compares hypothetical ideal pyroxenoids and pyroxenes – specifically the relationships between their tetrahedral and octahedral structural subunits, their anion packing arrangements, their octahedral arrangements, and the compositions of their "polyhedral layers", as defined below. The octahedral arrangement of a hypothetical pyroxenoid with T-chain repeat unit length of 11 is predicted. Finally, the new approaches are applied to see how yangite compares with the pyroxenoids and provide an understanding of why its structure is adopted.

Numerous papers have discussed the structural relationship between the pyroxenes and pyroxenoids, with a particular emphasis on the description of pyroxenoids as polysomes built from pyroxene and "wollastonite-like" (Angel and Burnham 1991) modules. By the 1980's, it was known that clinopyroxene (cpx) and pyroxenoid (pxd) intergrowths take place along face poles (1 -1 -1) and (0 0 1) in cpx and pxd, respectively (c.f. Ried 1984). During that decade, the existence of isostructural portions of the two structures that would allow seamless intergrowth was debated. By the early 1990's, it was determined that such portions did exist (c.f. Veblen

1991; Angel and Burnham 1991). Figures 1a and 1b illustrate isostructural planar portions of diopside (Thompson and Downs 2008) and rhodonite (Peacor et al. 1978), looking down face poles (1 -1 -1) and (0 0 1), respectively.

Many other discussions of the relationship between the pyroxenes and pyroxenoids focus on tetrahedral chain (T-chain) geometry and repeat length because T-chain repeat length in described pyroxenoids is variously 3, 5, 7, or 9 (c.f. Klein and Dutrow 2008). Prewitt and Peacor (1964) and Liebau (1956) noted that octahedral cation size determines T-chain type, with decreasing cation size corresponding to increasing T-chain repeat unit length. These topics will be addressed in detail later in the paper. Ohashi and Finger (1978) concluded that the distribution of octahedral cations between the different sites within the octahedral layers determine both structure type and the range of solid solutions. Both Prewitt and Peacor (1964) and Ohashi and Finger (1978) described pyroxenoids as having distorted closest-packed arrangements of oxygen anions.

This report analyzes pyroxenoids and pyroxenes in terms of several different structural subunits, defined here. For the purposes of this paper, a polyhedral layer is a unit that is one polyhedron thick in one direction, called the "stacking vector", and infinite in dimension in all directions perpendicular to the stacking vector. Layered structures, such as the pyroxenoids and pyroxenes, can be described as composed of one or more types of polyhedral layer stacked along the stacking vector in a finite sequence that repeats infinitely. Polyhedral layers can be used to orient related structures for comparison.

This approach is a natural extension of the concept that some crystal structures are based on close-packing of oxygen atoms. The polyhedral layers described below for diopside (and all clinopyroxenes) each consist of cations sandwiched between two adjacent close-packed oxygen

monolayers (Thompson and Downs 2003). Similarly, the pyroxenoid polyhedral layers analyzed in this paper consist of cations between two adjacent oxygen monolayers, although we will present evidence that these monolayers should not be considered close-packed. Selecting polyhedral layers that are bounded by oxygen monolayers (close-packed or not) constrains them to be one polyhedron in thickness and to consist of polyhedra that each have at least one "basal face", a face approximately parallel to the polyhedral plane (perpendicular to the stacking vector).

Figure 2 is a cartoon of diopside (Thompson and Downs 2008), wollastonite-1*A* (Ohashi and Finger 1978), and yangite (Downs et al. this issue) viewed perpendicular to their stacking vectors (looking at the polyhedral layers edge on) to illustrate the best alignment of the structures for comparison. This view is chosen so that the "tilt" of the octahedra (c.f. Thompson 1970, Papike et al. 1973, Thompson and Downs 2003) in each of the structures is evident and in alignment.

From this perspective, the layered nature of the structures is obvious, with five polyhedral layers visible in each representation. Each polyhedral layer in diopside, wollastonite, and the other well-known pyroxenoids analyzed in this paper contains either octahedra or tetrahedra, but not both. Such layers are hereafter referred to as "isopolyhedral layers". Layers such as those in yangite that contain more than type of polyhedron will be referred to as "mixed polyhedral layers".

Figure 3 is a cartoon of yangite viewed down **b**. From this angle, the structure could be considered to be constructed from alternating layers of tetrahedra and octahedra. However, these layers do not fit our definition of polyhedral layer because they are undulating and therefore more than one polyhedron thick, are not bounded by oxygen monolayers, contain polyhedra

96 without basal faces, and do not provide a natural basis for comparison with pyroxenes and
97 previously described pyroxenoids.
98 This study also uses idealized models of the octahedral layers of pyroxenes and
99 pyroxenoids to highlight similarities and differences instead of polysomatic construction or T-
100 chain geometry. Octahedral layers in pyroxenoids are composed of linear structural subunits that
101 are several octahedra wide and infinitely long. Prior authors (c.f. Weber 1983) have referred to
102 these edge-sharing arrangements as "bands", and this paper continues that practice.
103 Additionally, we will specifically focus on a single edge-sharing octahedral chain
104 (referred to hereafter as the "O-chain") interior to the octahedral band in each of
105 $Ca_{0.96}Mn_{0.04}SiO_3$ wollastonite-1*A* (Ohashi and Finger 1978), $Mn_{0.71}Mg_{0.17}Ca_{0.12}SiO_3$ rhodonite
106 (Peacor et al. 1978), $Mn_{0.92}Mg_{0.08}SiO_3$ pyroxmangite (Zanazzi et al. 2008), and $FeSiO_3$ ferrosilite
107 III (Weber 1983). Figures 4a-d illustrate the O-chains within the band of octahedra in each of
108 these minerals. Figure 5 isolates and idealizes the chains, placing them adjacent to each other to
109 highlight the stepwise progression from wollastonite through the other pyroxenoids towards the
110 pyroxene configuration.
111 Analyzing the O-chain instead of the entire octahedral band makes it easier to focus on
112 the key patterns and differences among these pyroxenoids. It also allows direct comparison
113 between each of the pyroxenoids and the pyroxene O-chain by placing them in the context of a
114 fully occupied, closest-packed sheet of idealized octahedra, hereafter referred to as a "brucite-
115 type layer", following common practice. Finally, it allows us to define the "single chain T:O
116 ratio" as the ratio of the length of the T-chain repeat length to the O-chain repeat length, a useful
117 parameter.

This study begins with a focus on wollastonite-1*A* (Ohashi and Finger 1978), for which we present a complete idealized hypothetical crystal structure data set, because of its relative simplicity in the sense that it contains only isopolyhedral layers, because its octahedral band geometry is comparatively straightforward as detailed below, and because its T-chain repeat length is the pyroxenoid minimum of three. It is also an end-member composition in the chemical continuum of crystals with general formula MXO_3, where the M-site(s) are occupied by one or more of a number of different metallic elements and X-site elements can be C, Si, Ge, B, or Al in either tetrahedral or trigonal coordination. End member compositions are particularly useful because they help elucidate the role of cation size in determining structure.

Discussion

Pyroxenoids are often described as similar to the pyroxene group because both groups contain chains of corner-sharing SiO_4 tetrahedra connected to chains of octahedrally coordinated cations, but distinguished by their T-chain geometry (c.f. Klein and Dutrow 2008). Specifically, pyroxenoid T-chains have a repeat unit that is three or more tetrahedra long, as opposed to the two-tetrahedra periodicity in pyroxenes (c.f. Merlino and Bonaccorsi 2008).

However, the pyroxene and pyroxenoid structures are fundamentally different in several other respects, including O-chain geometry, anion packing, and the relationship between their T- and O-chains. Tables 1 and 2 contain cell and positional parameters for a hypothetical ideal wollastonite-1*A* with the *C*-1 structure of Ohashi and Finger (1978), but constrained to have regular octahedra and T3 tetrahedron (the ideal T-site cation corresponding to the observed Si3 atom – Figure 6). These requirements fix the positions of all oxygen atoms except Oc1 [see Figure 6 – oxygen atom names follow Ohashi and Finger (1978), which will be the reference for observed wollastonite hereafter]. Oc1 is placed so all oxygen atoms form coplanar layers

stacked perpendicular to **a***, and T1 and T2 have identical geometries. While this choice is arbitrary, there is no placement of Oc1 that would result in a complete structure with all regular polyhedra, as would be the case if the anion skeleton of wollastonite were a distorted close-packed arrangement. This hypothetical idealized wollastonite will be used for comparison with observed wollastonite and ideal and observed diopside (Thompson and Downs 2008), arbitrarily chosen as a representative pyroxene.

Figure 6 is a cartoon of the relationship between the wollastonite-1*A* T-chains and O-chains, which are composed of a single type of octahedron (M3), illustrated for observed and ideal wollastonite viewed down **a*** and for the most analogous portion of a hypothetical closest-packed crystal. It is evident that there is no closest-packed model that directly corresponds with the wollastonite structure. Closest-packing creates characteristic arrangements of tetrahedral and octahedral interstitial sites. If the cation coordination polyhedra in a mineral cannot be mapped to corresponding sites in a closest-packed arrangement with an identical bonding topology, the mineral should not be considered as having a close-packed arrangement of anions.

By inspection of Figure 6, the single chain T:O ratio is three tetrahedra in the T-chain for every two O-chain octahedra, but in a close-packed mineral (like pyroxene – Thompson 1970; Thompson and Downs 2003) this ratio is 1:1. This creates an unusual geometry for T1 and T2 in the ideal wollastonite. T3 shares edges with M1 and M2 octahedra, and constraining the octahedra to be regular constrains T3 geometry to also be regular. Therefore, the mismatch in the single chain T:O ratio relative to closest-packing (which allows all polyhedra to be regular) must be accommodated by T1 and T2 in the hypothetical structure, and they deviate markedly from regular.

In reality, Si tetrahedra are extremely resistant to distortion and in observed wollastonite the octahedral sites Ca1 and Ca2 are quite distorted allowing T-sites Si1 and Si2 to be nearly regular. Si3 is the most distorted tetrahedron, but is still more regular than M3 and much less distorted than M1 and M2.

Figure 7 shows a view down **a*** of the bridging tetrahedra in observed and ideal wollastonite along with the O-chains that they connect. It also illustrates a portion of a hypothetical closest-packed crystal with occupancies chosen to provide the nearest possible correspondence to the wollastonite diagrams. Si_3 bridges Si_1 and Si_2 (Figure 6) but is not shown so that the octahedra are fully visible. Taking into account the missing Si_3, there are 3 tetrahedra in the T-chain for every 2 octahedra in the adjacent octahedral chains, 1 more than is possible in a closest-packed arrangement.

It is evident that the octahedra are distorted to accommodate the extra T site. The two pictured O-chains are composed of alternating M1 and M2 sites. Table 3 contains polyhedral angle variance values for the polyhedra in observed wollastonite, a traditional measure of polyhedral distortion (Robinson et al. 1971) such that a regular polyhedron has a value of 0 and larger values indicate greater distortion. Table 3 shows that Ca1 and Ca2 are much more distorted than Si1 and Si2, accommodating the high T:O ratio.

Additionally, Figure 7 again demonstrates that there is no closest-packed model that directly corresponds with the wollastonite structure.

While any idealized pyroxenoid O-chain taken in isolation can be placed into a brucite-type layer (see below), two or more idealized octahedral bands cannot without altering their relative positions. Figure 8 is a cartoon of a portion of an ideal wollastonite octahedral layer viewed down **a***. The darker octahedra are M3 and the dotted arrows indicate a minimum

translation the lower octahedral band would have to undergo relative to the upper octahedral band in order to be closest-packed.

We now compare and contrast the pyroxenoid and pyroxene O-chains by placing them in the context of a closest-packed brucite-type octahedral layer.

Figure 6 included the M3 O-chain in observed and ideal wollastonite; Figure 9a illustrates the M1 O-chain in observed and ideal diopside, looking down **a*** with the O-chains running parallel to **c**. Figure 9b illustrates the relationship between the wollastonite and pyroxene O-chains by placing them in the context of a brucite-type layer. There are three ways to orient a pyroxene O-chain in a brucite-type layer relative to a wollastonite O-chain: two with pyroxene **c** axis at 30° to the wollastonite **c** axis and one with the axes perpendicular. Figure 9b shows one of the 30° orientations – the other two may be easily visualized from figures 9a and 9b. These differences are fundamental because they determine how T-chains can be oriented relative to O-chains in close-packed minerals.

O-chains in more complex but still isopolyhedral layer pyroxenoids can be thought of as intermediate between the endmember O-chains of wollastonite and pyroxene. Figures 10a-c illustrate the relationships between the pyroxene and pyroxenoid O-chains for rhodonite (Peacor et al. 1978), pyroxmangite (Zanazzi et al. 2008), and ferrosilite III (Weber 1983), which have T-chain repeat lengths of 5, 7, and 9, respectively, by placing them in the context of brucite-type layers. Longer T-chain repeat unit lengths correlate with O-chain geometries that are increasingly pyroxene-like. Each time the pyroxenoid T-chain repeat length increases by 2, the number of octahedra overlapping between the pyroxene and pyroxenoid O-chains increases by 2.

As O-chain geometries become increasingly pyroxene-like with increasing T-chain repeat length, so do T:O single chain ratios in isopolyhedral layer pyroxenoids. Table 4 demonstrates

that the T:O ratio in these minerals is x:x - 1, where x is the T-chain repeat length. The T-chain repeat length increases by 2, the pyroxene T-chain repeat length, in each succeeding row in the table. Correspondingly, the O-chains become increasingly staggered in a fashion that makes them more pyroxene-like and the T:O ratio approaches the pyroxene value of 1:1.

In an ideal closest-packed structure, the octahedral:tetrahedral volume ratio is 4:1. In observed wollastonite, the average ratio is 7.7:1. The large size of the Ca atom is responsible for this large volume ratio, and the large size of the octahedra allows for the 3:2 single chain T:O ratio. The difference in the T:O ratio between pyroxenes and pyroxenoids is a fundamental structural difference, and another proof that pyroxenoids are not close-packed minerals.

Table 5 lists average M-site cation radius and average O-chain cation radius for the four pyroxenoids discussed so far and for diopside. T-chain repeat length increases and the pyroxenoids become more pyroxene-like as average O-chain cation radius decreases. One can easily imagine a pyroxenoid structure falling in between ferrosilite III and clinopyroxene with the O-chain geometry illustrated in Figure 11 and a T-chain repeat unit of length eleven. These structures are related by straightforward intralayer alterations in chain geometry resulting from differences, sometimes relatively small, in chemistry. Ferrosilite III is a high-temperature synthetic. A pyroxenoid with T-chain repeat length of 11 may not exist in nature, but it may be possible to synthesize such a crystal at high temperature if the starting materials contain the correct ratio of Fe and a smaller M cation such as Mg.

By the criteria of this discussion, amphiboles are much more like pyroxenes than are pyroxenoids because their O-chains can be oriented parallel to pyroxene O-chains in a brucite-type layer, they have the pyroxene T-chain repeat unit length of 2, and they have T:O ratios of 1:1 between T-chains and their associated octahedra.

All of the phases so far discussed have general formula $MSiO_3$ and have O-chain geometries that lie somewhere on the wollastonite-pyroxene spectrum. All contain isopolyhedral layers and form the well-known wollastonite-rhodonite-pyroxmangite-ferrosilite III-clinopyroxene series.

However, there is at least one pyroxenoid-like chain silicate that has a different stoichiometry and is related to wollastonite in a different fashion. The new mineral yangite has general formula $M1M2Si_3O_9$, and can be thought of as composed of mixed polyhedral layers that contain both T- and O-sites stacked along face pole (-1, 0, 3). Yangite's O-chains orient in a brucite-type layer in the same manner as wollastonite, but yangite's M:T formula ratio is two-thirds that of wollastonite and therefore has an octahedral band that is 2 octahedra wide instead of 3 as in wollastonite.

Yangite has two related complexities not present in the pyroxenoids discussed so far – double T-chains and layers that are not isopolyhedral. Figure 12a compares a portion of yangite viewed down **b** with a portion of wollastonite viewed down **c**, illustrating the mixed polyhedral layers of yangite vs. the isopolyhedral layers of wollastonite. Yangite's double T-chain connects four octahedral bands of width 2 in four different layers, while wollastonite's single T-chain connects three octahedral bands of width 3 in two different layers.

The two halves of yangite's double T-chains are related by an inversion, making them very different geometrically from amphibole double T-chains, which are related by a mirror. The inversion splits the double chain between polyhedral layers, resulting in the mixed polyhedral layers described above (Figure 12a). To visualize this, compare the yangite double T-chains (Figure 12a) with the top half of Figure 12b, which illustrates the amphibole double T-chain using obertiite (Hawthorne et al. 2000) as an exemplar.

Each half of the yangite double T-chain (i.e. each component single chain) performs the same structural function as the pyroxenoid single T-chain, the pyroxene single T-chain, and the amphibole double T-chain. Each of these components connects to 2 linear structural subunits in one of the adjacent polyhedral layers and to 1 in other adjacent polyhedral layer. In the case of the pyroxenoids, pyroxenes, and amphiboles, these linear subunits are all octahedral bands. In the case of yangite, one of them is a single T-chain (half of the double T-chain). To see this, imagine removing the uppermost and rightmost octahedral bands in Figure 12a's yangite illustration. With that image in mind, the central T-chain in all four of Figure 12's diagrams is functionally the same.

Yangite exhibits the 3:2 single chain T:O ratio characteristic of wollastonite along with its T chain repeat length of 3. Figure 13 illustrates this similarity. It also highlights an important difference between yangite and wollastonite: the orientation of the yangite T-chain relative to its associated O-chain is opposite that of wollastonite. To see this, observe that the visible face of the yangite T3 tetrahedron and the approximately parallel faces of its two associated octahedra point in opposite directions; but in wollastonite, the visible T3 tetrahedral face points in the same direction as the parallel face of its associated octahedron.

Pyroxenes and pyroxenoids are often described as composed of interconnected “I-beams” (c.f. Papike et al 1973), a structural subunit consisting of an octahedral band sandwiched between two single-T chains. Figure 14 contrasts the yangite and wollastonite-1*A* I-beams. There are important differences between the manner in which I-beams are connected in the two minerals. The yangite I-beam is connected to 4 other I-beams and has a T-T connection (to the other half of the double T-chain), while the wollastonite I-beam is connected to 6 other I-beams and only through T-O connections. The yangite I-beams connects to other I-beams through

bridging oxygens, but the wollastonite octahedral band shares edges with some tetrahedra in other I-beams. Yangite has no connections to other I-beams at the northeast and southwest corners of the octahedral band pictured in Figure 14, while the wollastonite octahedral band is connected at all 4 corners.

These differences are evident in Figure 15, which shows how the octahedral bands connect to other I-beams at the northwest and southeast corners as pictured in Figure 14. The tetrahedra in Figure 15 belong to neighboring I-beams and not the I-beam that includes the pictured octahedral band, whose tetrahedra have been removed from the image. Each illustrated T-chain segment contains 2 three-tetrahedron repeat units. The opposite orientation of the T-chains relative to the octahedral bands in yangite and wollastonite described above is again evident here and requires different I-beam connectivity.

Definitions of the term "pyroxenoid" often include a single T-chain as a defining characteristic. This definition precludes yangite from classification as a pyroxenoid. Yangite and the pyroxenoids bear more similarity to each other than either does to any other mineral species or group. Reasonable arguments could be made to expand the definition of "pyroxenoid" so that it includes yangite, coin the term "amphiboloid" and count yangite as this new group's first member (as suggested by one reviewer), or leave it on its own.

Downs et al. (this issue) present yangite in a setting that corresponds with the predicted structure of Merlino and Bonaccorsi (2008), and this is the setting used in this paper's figures. The conventional settings for pyroxenes and pyroxenoids puts **c** parallel to the octahedral bands and T-chains and the stacking vector parallel to **a***. A large cell is required to place yangite in a corresponding setting, with cell parameters [**a'**, **b'**, **c'**, α', β', γ'] = [c, 3a + b + c, b, acos([311] • **b** / |[311]| × b), α, acos([311] • **c** / |[311]| × c)] and positional parameters [x', y', z'] = [-x/3 + z, x/3,

-x/3 + y]. A simpler transformation, [**a'**, **b'**, **c'**, **α'**, **β'**, **γ'**] = [c, a, b, γ, α, β] and [x', y', z'] = [z, x, y], puts **c** parallel to the octahedral bands and T-chains, but doesn't put the stacking vector parallel to **a***, and therefore isn't as useful for structural comparisons.

Yangite was refined without locating the hydrogen atoms (Downs et al. this issue). The refinement leaves O9W dangling, bonded only to Mn (Figure 16), an extremely unusual topology. The fact that O9W is a water molecule may be enough to stabilize the structure, but the presence of hydrogen bonds is likely. Any such hydrogen bonds cannot be located with certainty, but a range of possibilities can be described.

Procrystal electron density calculations (c.f. Downs et al. 2002 for a description of the method and its efficacy) indicate weak O9W-O2, O9W-O3, O9W-O9W, O9W-Pb bonds (Downs et al. this issue). Figure 16 illustrates these bond paths. There are two more bonds than hydrogen atoms because stabilizing O-O bonds may exist without the presence of hydrogen bonding (c.f. Pakiari et al. 2007). We rule out the O9W-O9W bond path as a location for hydrogen atoms because a single hydrogen along this path violates the crystal's symmetry. Although stabilizing H-H bonds for nearly electrically neutral hydrogen atoms in organic molecules have been reported (Matta et al. 2003), we also rule out two hydrogen atoms along the O9W-O9W path based on crystal chemistry.

There are three remaining possible pairs of hydrogen bonds: O9W-O2 and O9W-O3, O9W-O2 and O9W-Pb, or O9W-O3 and O9W-Pb, with no solid criteria for choosing among them. The O9W-Pb bond path is an intriguing possibility given lead's lone pair of electrons. Unfortunately, there is not enough yangite sample to propose a neutron diffraction study to locate its hydrogen atoms, but the possibility of an O-Pb hydrogen bond is sufficiently

interesting that a search for a similar crystal chemical environment in a more abundant compound is worthwhile.

Implications

Several lines of evidence demonstrate that while pyroxenes are based on close-packing of oxygen atoms, pyroxenoids are not. This is a profound structural difference and is the result of the characteristic pyroxenoid T-chain/O-chain geometry. Specifically, every pyroxenoid T- and associated O-chain contains at least a segment in which the T:O single chain ratio is 3:2, a geometry incompatible with close-packing. Pyroxenoid packing arrangements and relationships with pyroxenes cannot be fully understood through T-chain analysis alone; O-chain geometries provide fundamental insights because O-chain chemistry varies between pyroxenoids while T-chains are always composed of SiO_4 tetrahedra.

Because the octahedral chains of both pyroxenes and pyroxenoids can be placed in the context of a close-packed brucite-type layer, O-chains are ideal for analyzing the relationships between pyroxenes and pyroxenoids. Such analysis shows that as the average O-chain cation size decreases, O-chain geometry (and therefore the T:O single chain ratio) becomes increasingly staggered and pyroxene-like in predictable fashion. One can therefore easily predict what the O-chain in an isopolyhedral layer pyroxenoid with T-chain repeat length 11 (or more) will look like if and when such a mineral is discovered or crystal synthesized.

Additionally, because octahedral bands in pyroxenoids when considered in isolation have close-packed arrangements of oxygens, they must distort considerably to accommodate the non-closest-packed T-chains that they are connected to.

The existence of a pyroxenoid-like crystal with mixed polyhedral layers, yangite, suggests that the number of possible structures closely related to the pyroxenoids is much larger

than previously thought and that new minerals with novel related structures will continue to be discovered.

Pyroxenoids can be classified in several new ways: O-chain geometry, single chain T:O ratios, mixed vs. isopolyhedral layers, and single vs. double (or perhaps more) T-chains.

Acknowledgments

We thank an anonymous reviewer, Dr. Fernando Cámara, and Associate Editor Dr. Fernando Colombo, whose comments greatly improved the quality of this manuscript. We particularly appreciate Dr. Cámara's extensive edit and the time it must have required.

References

Angel, R.J., and Burnham, C.W. (1991) Pyroxene-pyroxenoid polysomatism revisited: a clarification. American Mineralogist 76, 900-903.

Downs, R.T., Gibbs, G.V., Boisen, M.B. Jr., and Rosso, K.M. (2002) A comparison of procrystal and ab initio model representations of the electron-density distributions of minerals. Physics and Chemistry of Minerals 29, 369-385.

Downs, R.T., Pinch, W.W., Thompson, R.M., Evans, S.H., and Megaw, L. (2016) Yangite, $PbMnSi_3O_8 \cdot H_2O$, a new mineral species with double wollastonite silicate chains, from the Kombat mine, Namibia. American Mineralogist x, y-z.

Hawthorne, F.C., Cooper, M.A., Grice, J.D., and Ottolini, L. (2000) A new anhydrous amphibole from the Eifel region, Germany: Description and crystal structure of obertiite, $NaNa_2(Mg_3FeTiSi_8O_{22}O_2$. American Mineralogist 85, 236-241.

Klein, C., and Dutrow, Barbara (2008) *The Manual of Mineral Science*. John Wiley & Sons, Hoboken, New Jersey.

Liebau, F. (1956) Bemerkungen zur systematik der kristallstrukturen von silikaten

372 mit hochkondensierten anionen. Zeitschrift für physikalische Chemie 206, 73-92.
373 Matta, C.F., Hernández-Trujillo, J., Tang, T.-H., and Bader, R.F.W. (2003) Hydrogen-hydrogen
374 bonding: A stabilizing interaction in molecules and crystals. Chemistry – A European Journal
375 9, 1940-1951.
376 Merlino, S., and Bonaccorsi, E. (2008) Double wollastonite chains: topological/conformational
377 varieties, polytypic forms, isotypic compounds. Zeitschrift für Kristallographie 223, 85-97.
378 Ohashi, Y. and Finger, L.W. (1978) The role of octahedral cations in pyroxenoid crystal
379 chemistry. I. Bustamite, wollastonite, and the pectolite-schizolite-serandite series. American
380 Mineralogist 63, 274-288.
381 Pakiari, A.H., and Eskandari, K. (2007) Closed shell oxygen-oxygen bonding interaction based
382 on electron density analysis. Journal of Molecular Structure: THEOCHEM 806, 1-7.
383 Papike, J.J., Prewitt, C.T., Sueno, S., and Cameron, M. (1973) Pyroxenes: comparisons of real
384 and ideal structural topologies. Zeitschrift für Kristallographie, 138, 254-273.
385 Peacor, D.R., Essene, E.J., Brown, P.E., and Winter, G.A. (1978) The crystal chemistry and
386 petrogenesis of a magnesian rhodonite. American Mineralogist 63, 1137-1142.
387 Prewitt, C.T., and Peacor, D.R. (1964) Crystal chemistry of the pyroxenes and pyroxenoids.
388 American Mineralogist 49, 1527-1542.
389 Ried, H. (1984) Intergrowth of pyroxene and pyroxenoid; chain periodicity faults in pyroxene.
390 Physics and Chemistry of Minerals 10, 230-235.
391 Robinson, K., Gibbs, G.V., and Ribbe, P.H. (1971) Quadratic elongation: a quantitative measure
392 of distortion in coordination polyhedra. Science 172, 567-570.
393 Shannon RD (1976) Revised effective ionic radii and systematic studies of interatomic distances
394 in halides and chalcogenides. Acta Crystallographica A32, 751-767.

395 Thompson, J.B. (1970) Geometrical possibilities for amphibole structures: model biopyriboles.
396 American Mineralogist, 55, 292-293.
397 Thompson, R.M., and Downs, R.T. (2003) Model pyroxenes I: ideal pyroxene topologies.
398 American Mineralogist 88, 653-666.
399 Thompson, R.M., and Downs, R.T. (2008) The crystal structure of diopside at pressure to 10
400 GPa. American Mineralogist, 93, 177-186.
401 Veblen, D.R. (1991) Polysomatism and polysomatic series: A review and application. American
402 Mineralogist 76, 801-826.
403 Weber, H.-P. (1983) Ferrosilite III, the high-temperature polymorph of $FeSiO_3$. Acta
404 Crystallographica C39, 1-3.
405 Zanazzi, P.F., Nestola, F., Nazzareni, S., and Comodi, P. (2008) Pyroxmangite: A high pressure
406 single-crystal study. American Mineralogist 93, 1921-1928.

Figure Legends

Figure 1a. Diopside (Thompson and Downs 2008) viewed down face pole (1 -1 -1).

Figure 1b. Rhodonite (Peacor et al. 1978) viewed down face pole (0 0 1).

Figure 2. The structures of diopside (Thompson and Downs 2008), wollastonite-1*A* (Ohashi and Finger 1978), and yangite (Downs et al. this issue) viewed so that "tilt" of the octahedra (c.f. Thompson 1970, Papike et al. 1973, Thompson and Downs 2003) in each of the structures is evident and in alignment.

Figure 3. Yangite viewed down **b**.

Figure 4. The edge-sharing "O-chain" in four pyroxenoids, each of which has different T-chain repeat length. The O-chain is interior to the octahedral band and is highlighted in Figures 2a-d as darker octahedra. (a) wollastonite-1*A* (Ohashi and Finger 1978), (b) rhodonite (Peacor et al. 1984), (c) pyroxmangite (Zanazzi et al. 2008), and (d) ferrosilite III (Weber 1983) have T-chain repeat lengths of 3, 5, 7, and 9, respectively.

Figure 5. Idealized versions with regular octahedra of the O-chains in wollastonite-1*A* (Ohashi and Finger 1978), rhodonite (Peacor et al. 1984), pyroxmangite (Zanazzi et al. 2008), ferrosilite III (Weber 1983), and pyroxene (Thompson and Downs 2003).

Figure 6. The relationship between the T- and O-chains in observed and ideal wollastonite-1*A*, viewed down **a***, and the most analogous portion of a hypothetical closest-packed crystal. There are three tetrahedra for every two octahedra with which the tetrahedra share apical corners, greater than the closest-packed ratio of 1:1 and a demonstration that wollastonite is not a close-packed mineral. Observed wollastonite is from Ohashi and Finger (1978).

Figure 7. A comparison of T1 and T2 bridging the O-chains in observed (Ohashi and Finger 1978) and ideal wollastonite-1*A*, viewed down **a***, and the most analogous portion of a

hypothetical closest-packed crystal. Si-tetrahedra are extremely resistant to distortion, and the octahedra in observed wollastonite distort to allow the tetrahedra to become more regular.

Figure 8. A portion of the ideal wollastonite-1*A* octahedral layer, viewed down **a***. M3 octahedra are darker. The arrows indicate a minimum translation necessary to make the layer closest-packed, again demonstrating that wollastonite is not a close-packed mineral.

Figure 9a. A comparison of the M1 O-chain in observed and ideal diopside (Thompson and Downs 2008) viewed down **a***, with the O-chain running parallel to **c**. Ideal diopside is constrained to have regular tetrahedra.

Figure 9b. The ideal wollastonite (labeled 'W') and diopside (labeled 'D') O-chains placed in the context of a fully occupied closest-packed octahedral layer (brucite-type layer). O-chain orientation in the brucite-type layer is important because it determines the possible orientations of associated T-chains in close-packed minerals.

Figure 10. The relationships between the pyroxene and pyroxenoid O-chains for (a) rhodonite (Peacor et al. 1978), (b) pyroxmangite (Zanazzi et al. 2008), and (c) ferrosilite III (Weber 1983), which have T-chain repeat lengths of 5, 7, and 9, respectively

Figure 11. The O-chain geometry in the context of a brucite-type layer of a hypothetical pyroxenoid with a T-chain repeat unit length of eleven.

Figure 12a. A comparison of yangite (Downs et al, this issue) viewed down **b** with wollastonite-1*A* (Ohashi and Finger 1978) viewed down **c**.

Figure 12b. A comparison of amphibole (obertiite – Hawthorne et al. 2000) with clinepyroxene (diopside – Thompson and Downs 2008), both viewed down **c**.

452 **Figure 13.** A comparison of half of the yangite double T-chain viewed down face pole (-1 0 3)
453 with the wollastonite T-chain (Ohashi and Finger 1978) viewed down **a*** showing their identical
454 tetrahedral geometries, but opposite orientations relative to the octahedra.
455 **Figure 14.** The I-beams of yangite (Downs et al, this issue) and wollastonite-1*A* (Ohashi and
456 Finger 1978).
457 **Figure 15.** Segments of the octahedral bands of yangite (Downs et al, this issue) and
458 wollastonite-1*A* (Ohashi and Finger 1978) along with T-chains from different I-beams.
459 **Figure 16.** A portion of the yangite structure viewed down **b**, showing possible hydrogen bonds
460 (dotted lines) bridging and perhaps stabilizing a channel in the structure.

Table 1. Cell parameters for a hypothetical ideal wollastonite with regular octahedra and the corresponding observed structure (Ohashi and Finger 1978). Ideal parameters are given exactly and as a decimal approximation. Exact parameters are expressed in terms of *r*, where *r* = one-half the octahedral edge length. Space group is C-1.

	Ideal wollastonite	*r* = 1.58982 Å	Ohashi and Finger (1978)
a (Å)	$2\sqrt{11}r$	10.546	10.104(1)
b (Å)	$(2/3)\sqrt{129}r$	12.038	11.054(1)
c (Å)	$4r$	6.359	7.305(1)
α (°)	$\cos^{-1}(-3/(2\sqrt{129}))$	97.59	99.53(1)
β (°)	$\cos^{-1}(-4/(8\sqrt{11}))$	98.67	100.56(1)
γ (°)	$\cos^{-1}(4/\sqrt{1419})$	83.90	83.44(1)
V(Å^3)	$416\sqrt{2}r^3/3$	788.0	788.0(1)

Table 2. Positional parameters for ideal and observed wollastonite. Ohashi and Finger (1978) did not report errors with their positions.

	Ideal	Ideal	O&F
M1	0	0	.0212
	19/26	.7308	.7800
	3/52	.0577	.0772
M2	0	0	.0180
	19/26	.7308	.7803

	29/52	.5577	.5712
M3	0	0	.0137
	1/2	.5	.4889
	1/4	.25	.2504
T1	3/16	.1875	.2265
	197/208	.9471	.9585
	173/208	.8317	.8876
T2	3/16	.1875	.2266
	197/208	.9471	.9576
	101/208	.4856	.4540
T3	3/16	.1875	.2260
	37/208	.1779	.1711
	45/208	.2163	.2237
Oa1	1/8	.125	.1164
	59/104	.5673	.5786
	5/104	.0481	.0381
Oa2	1/8	.125	.1168
	59/104	.5673	.5807
	57/104	.5481	.5612
Oa3	1/8	.125	.1149
	35/104	.3365	.3142
	77/104	.7404	.7305
Ob1	1/8	.125	.1248

	83/104	.7981	.8577
	89/104	.8558	.8750
Ob2	1/8	.125	.1239
	83/104	.7981	.8567
	37/104	.3558	.3657
Ob3	1/8	.125	.1147
	35/104	.3365	.2874
	25/104	.2404	.2271
Oc1	1/8	.125	.2201
	99/104	.9519	.9955
	67/104	.6442	.6780
Oc2	1/8	.125	.1811
	11/104	.1058	.0887
	45/104	.4327	.3703
Oc3	1/8	.125	.1823
	11/104	.1058	.0912
	97/104	.9327	.0119

470

471

Table 3. Polyhedral angle variance (Robinson et al. 1971) values for Ca1, Ca2, T1, and T1 in observed wollastonite (Ohashi and Finger 1978). A value of zero indicates a regular polyhedron, higher values indicate increasing distortion. The O-sites are much more distorted than the T-sites.

Site	Ca	Si
1	176.8	26.2
2	177.1	22.1
3	95.7	60.0

Table 4. The single chain T:O ratio in several isopolyhedral layer pyroxenoids. As the T-chain repeat length increases, the ratio approaches the pyroxene value of 1:1.

Mineral	T-chain repeat length	T:O	Reference
wollastonite	3	3:2	Ohashi and Finger, 1978
rhodonite	5	5:4	Peacor et al., 1978
pyroxmangite	7	7:6	Zanazzi et al., 2008
ferrosilite III	9	9:8	Weber, 1983
	x	x: x - 1	
diopside	2	1:1	Thompson and Downs, 2008

Table 5. The single chain T:O ratio in several isopolyhedral layer pyroxenoids. As the T-chain repeat length increases, the ratio approaches the pyroxene value of 1:1. Average M-site cation radius is calculated assuming 6-coordination. Radii are from Shannon (1976).

Mineral	T-chain repeat length	Ave. M-site cation radius (Å)	Ave. O-chain cation radius (Å)	Reference
wollastonite	3	0.99	0.99	Ohashi and Finger, 1978
rhodonite	5	0.83	0.85	Peacor et al., 1978
pyroxmangite	7	0.82	0.79	Zanazzi et al., 2008
ferrosilite III	9	0.78	0.78	Weber, 1983
diopside	2	0.86	0.72	Thompson and Downs, 2008

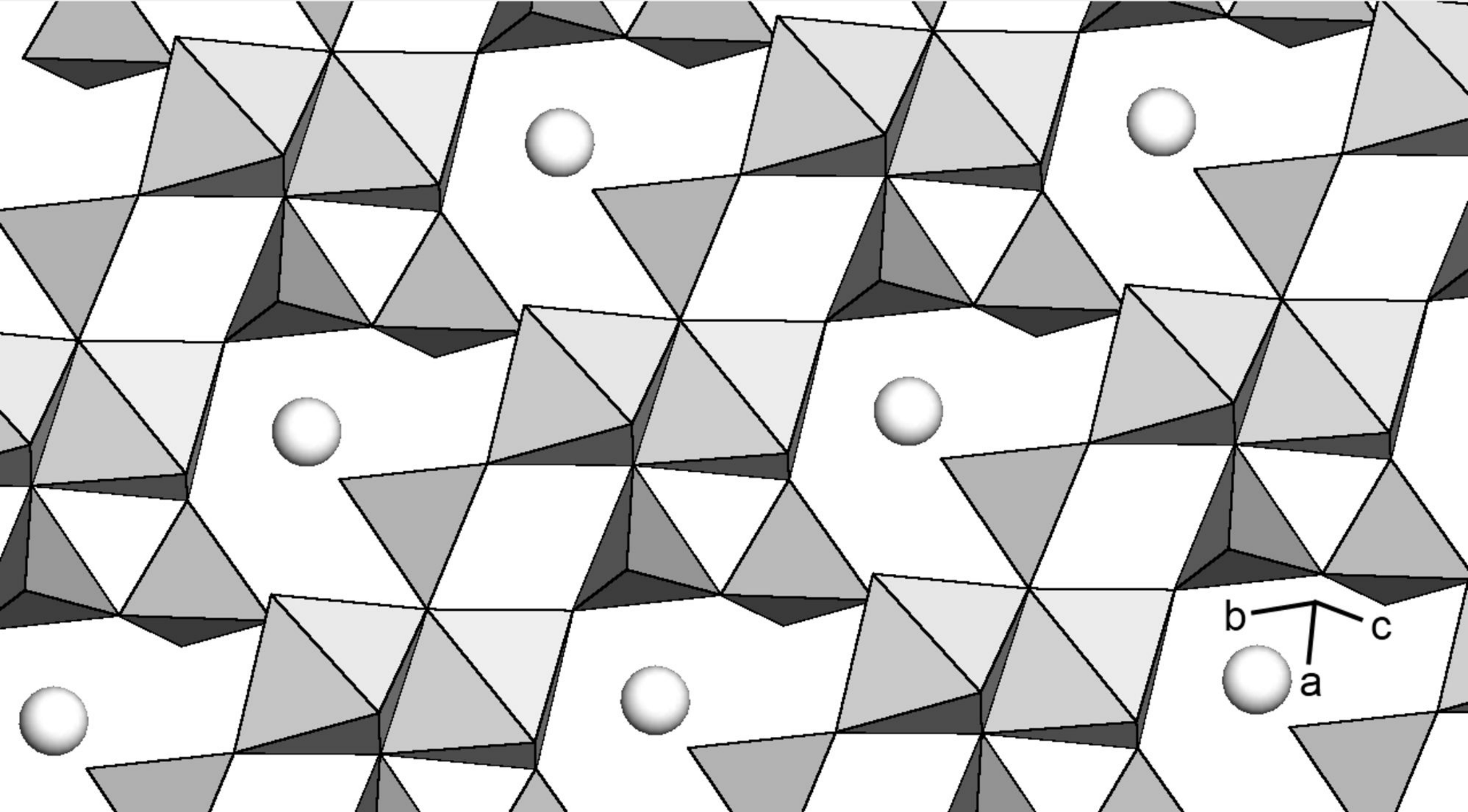
b
c
a

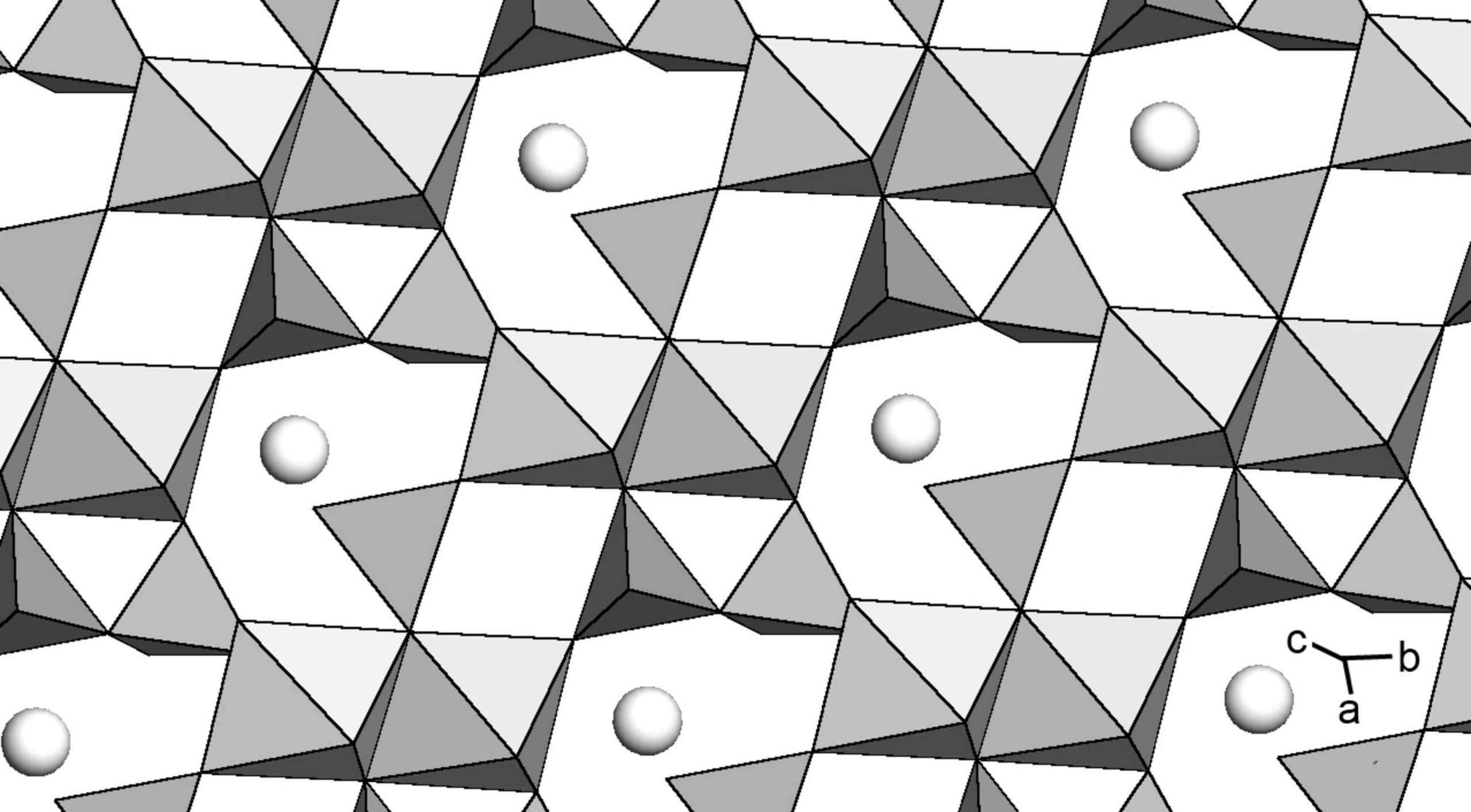
c
b
a

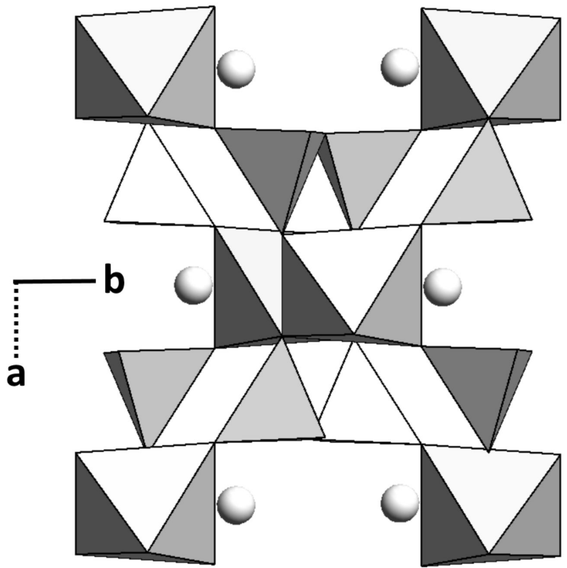

Diopside

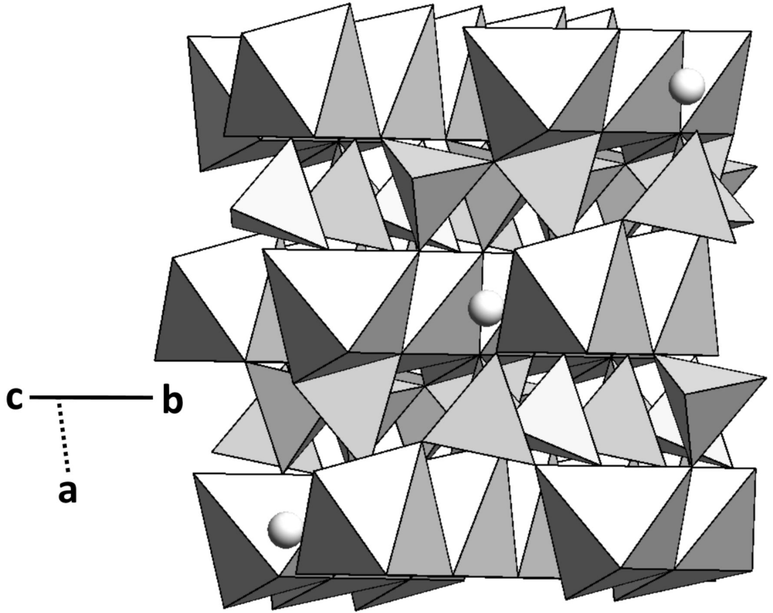

Wollastonite-1A

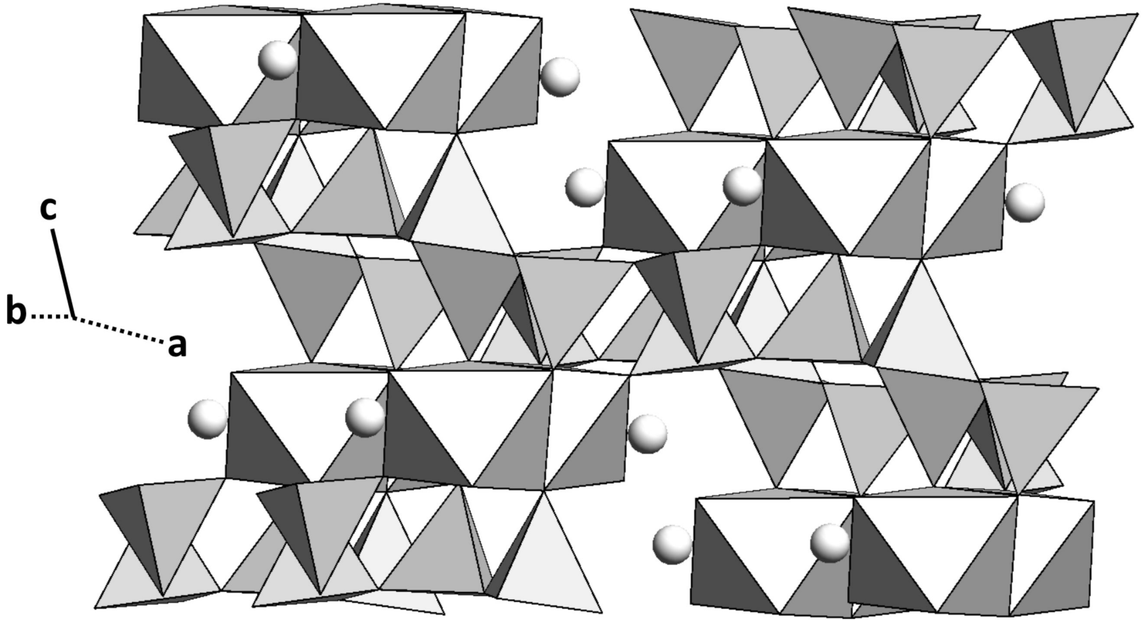

Yangite

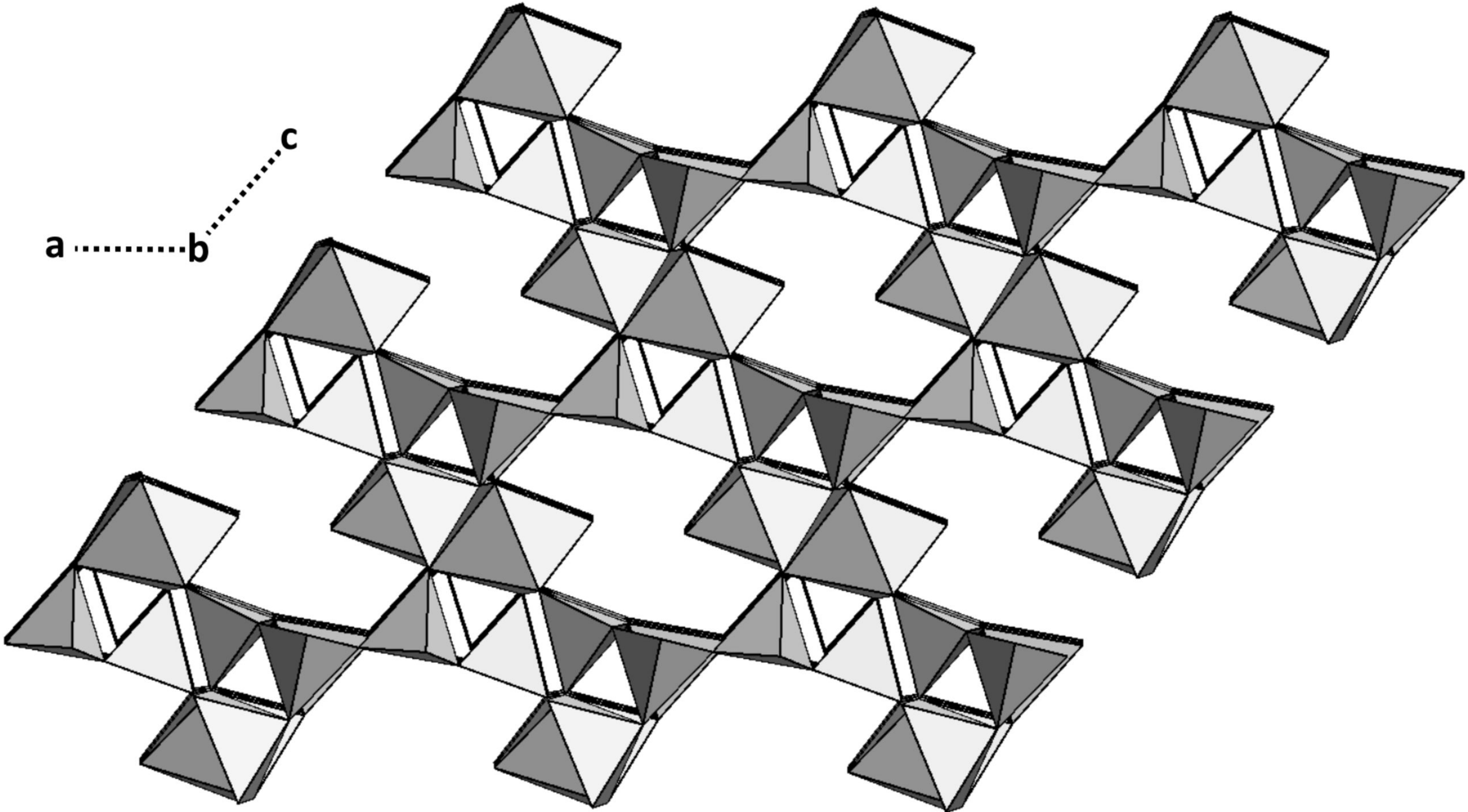
c
a
b

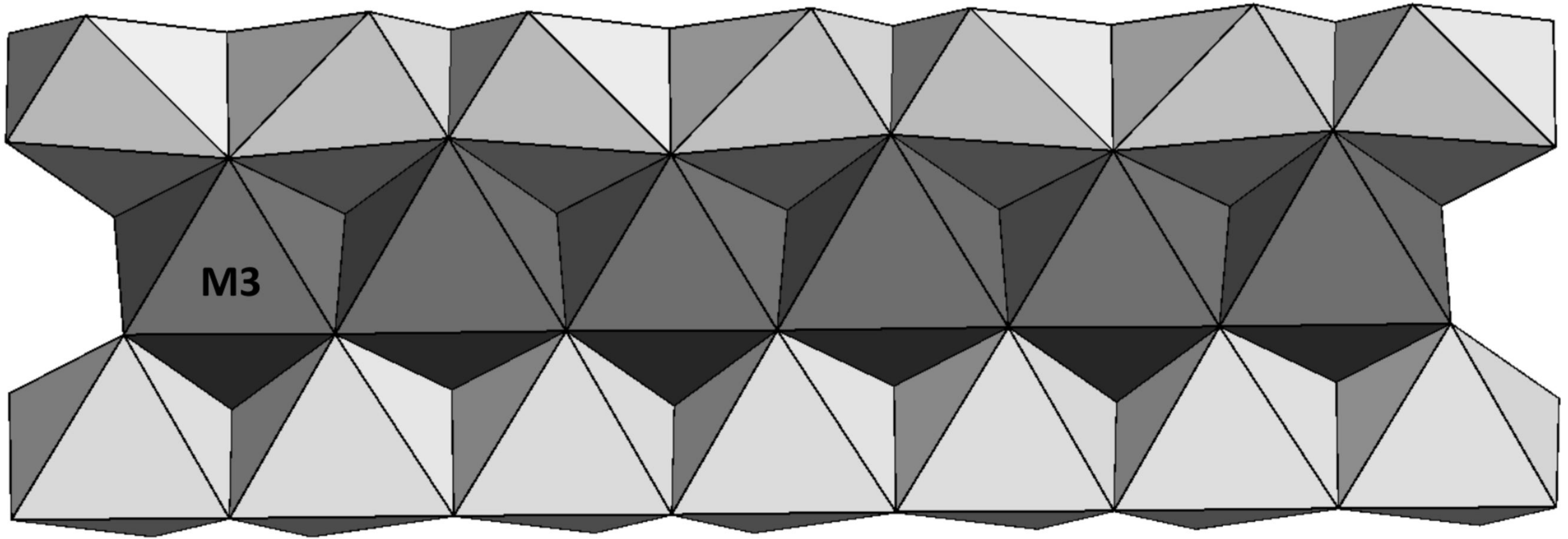

Wollastonite-1A

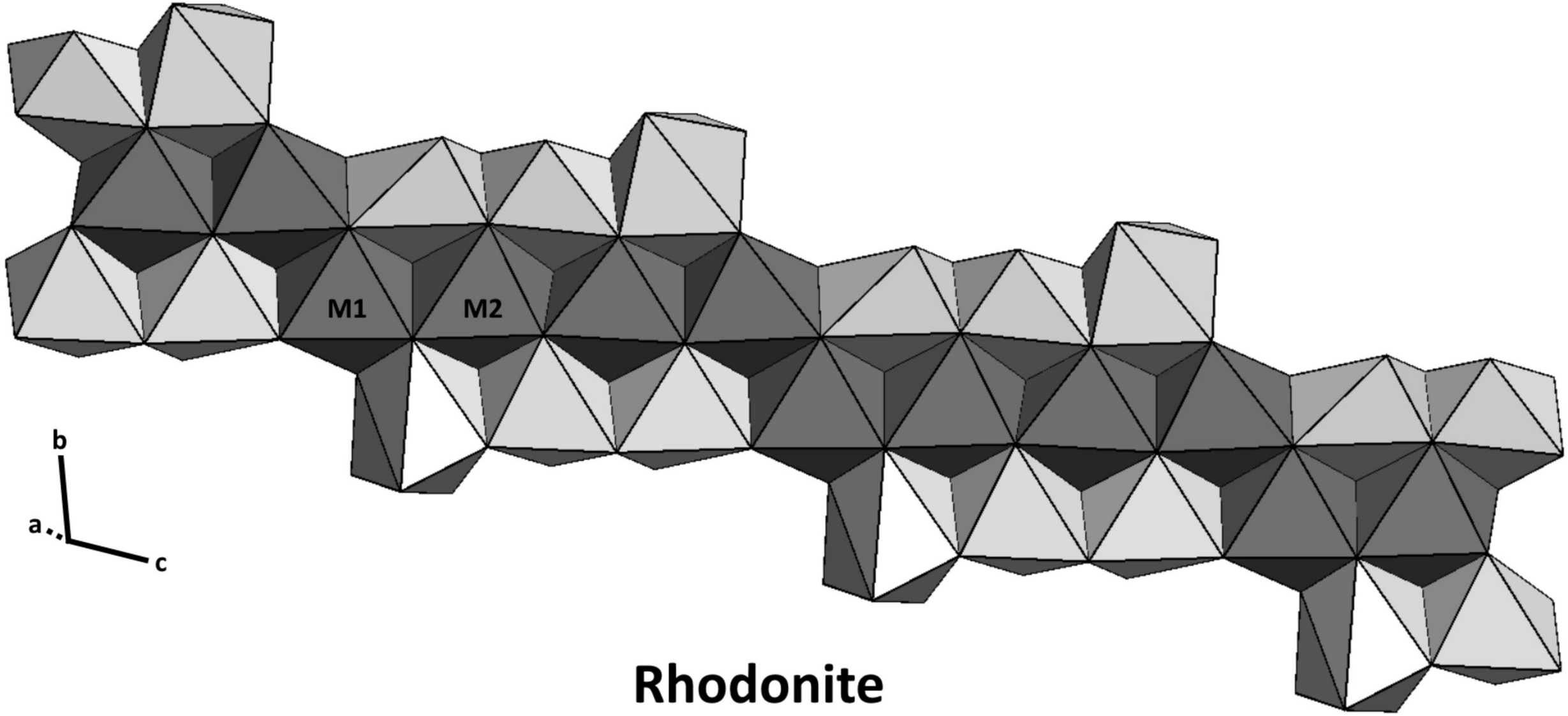

Rhodonite

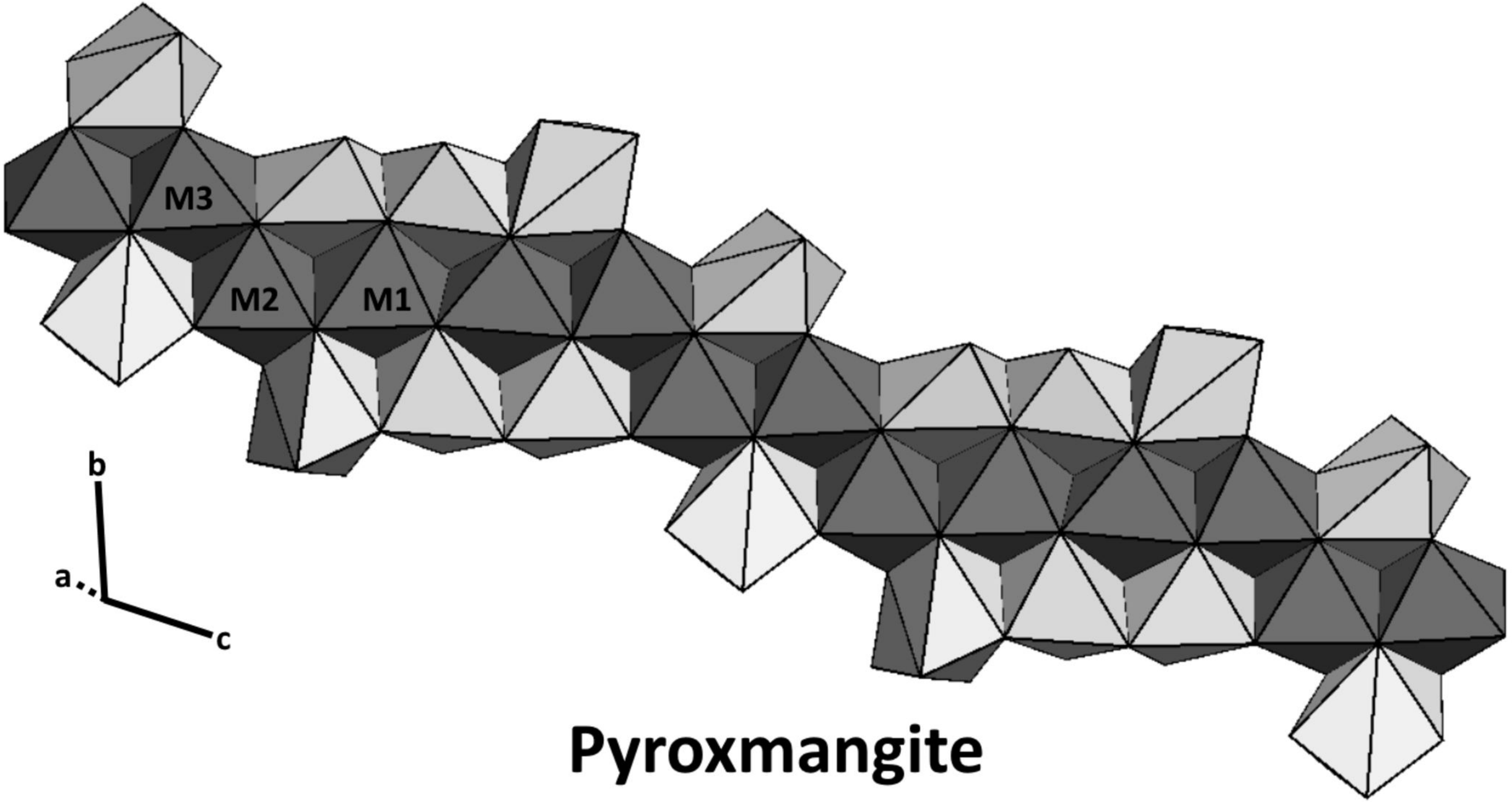

Pyroxmangite

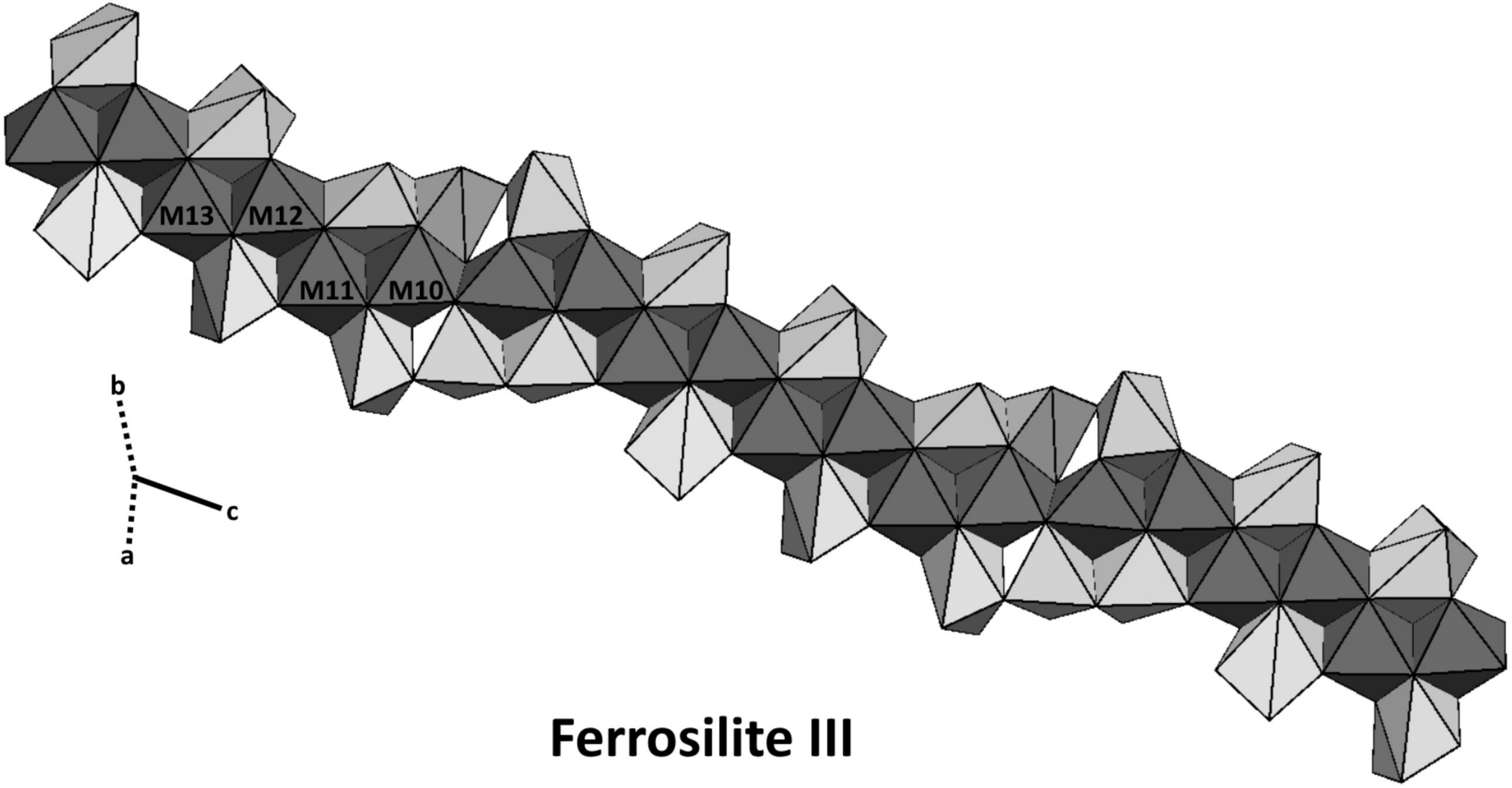

Ferrosilite III

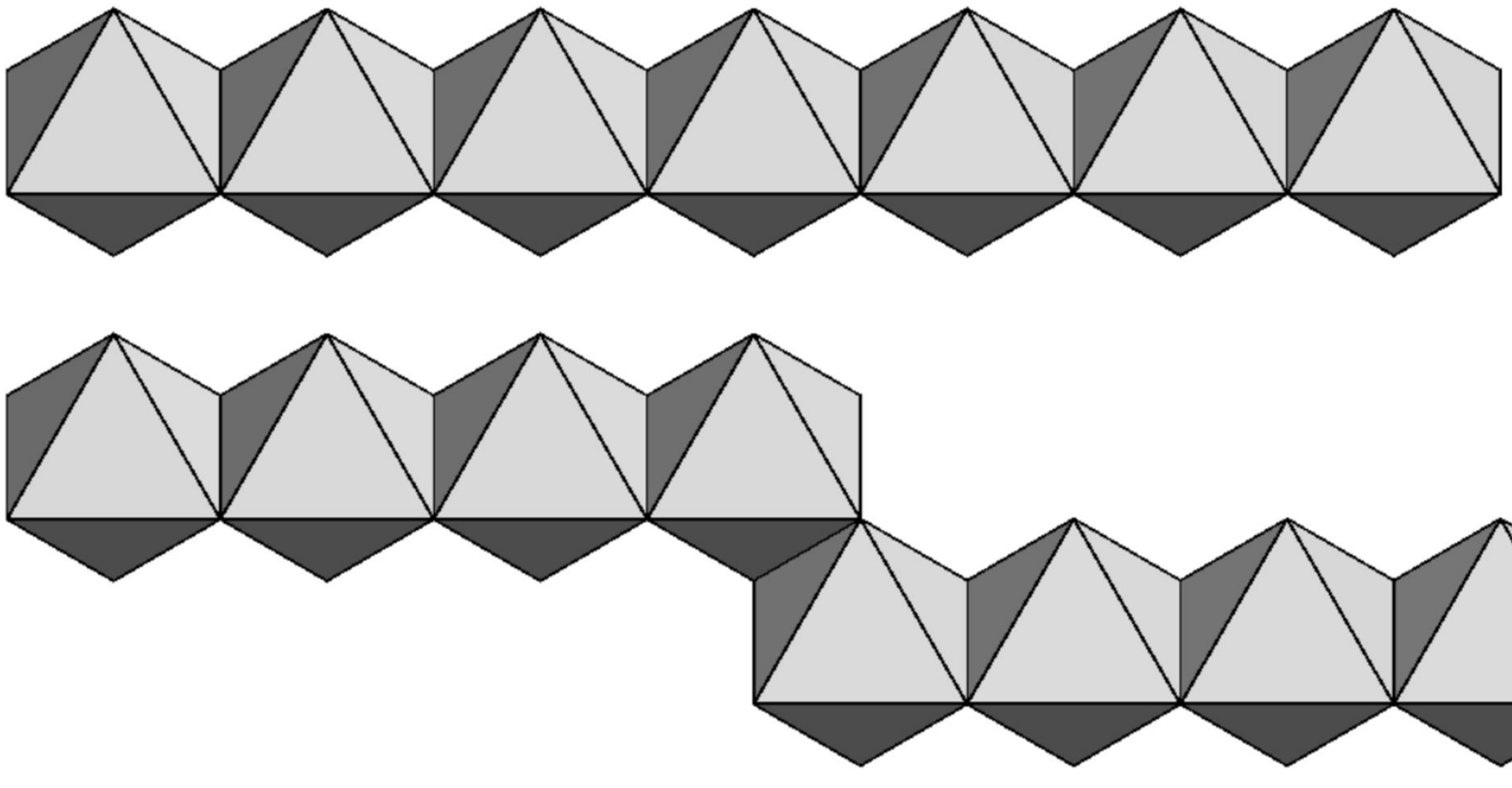

Idealized Octahedral Chains of Pyroxenoids and Pyroxene

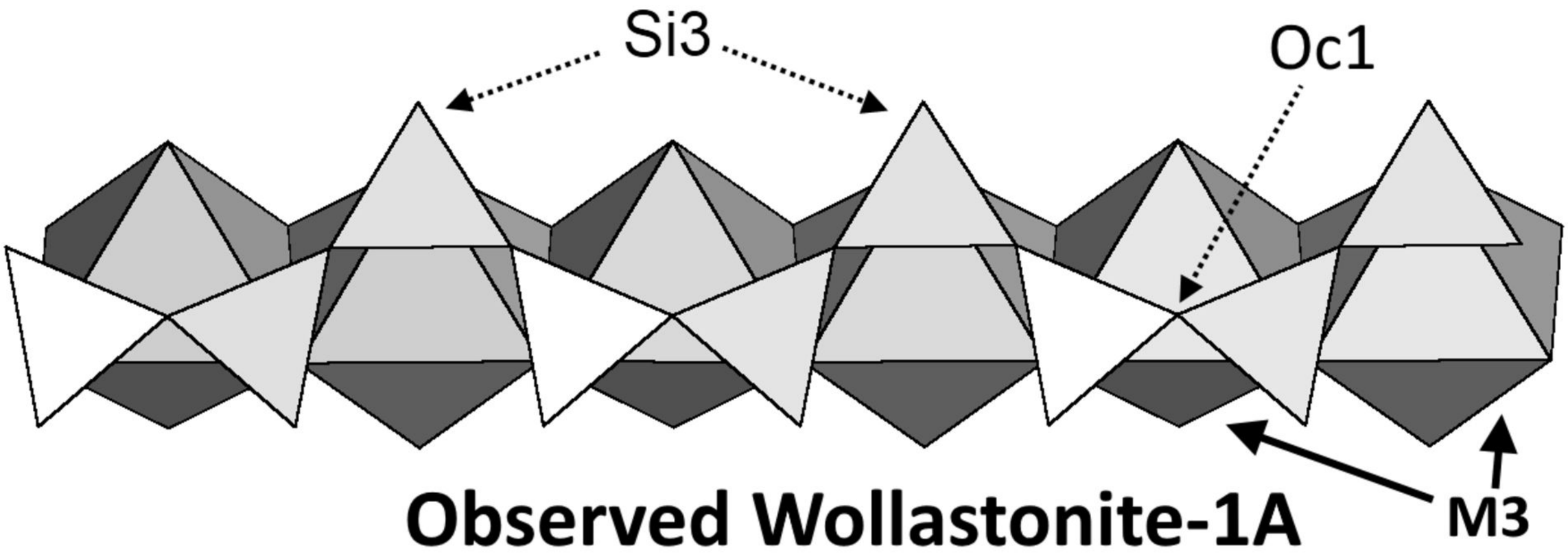

Observed Wollastonite-1A

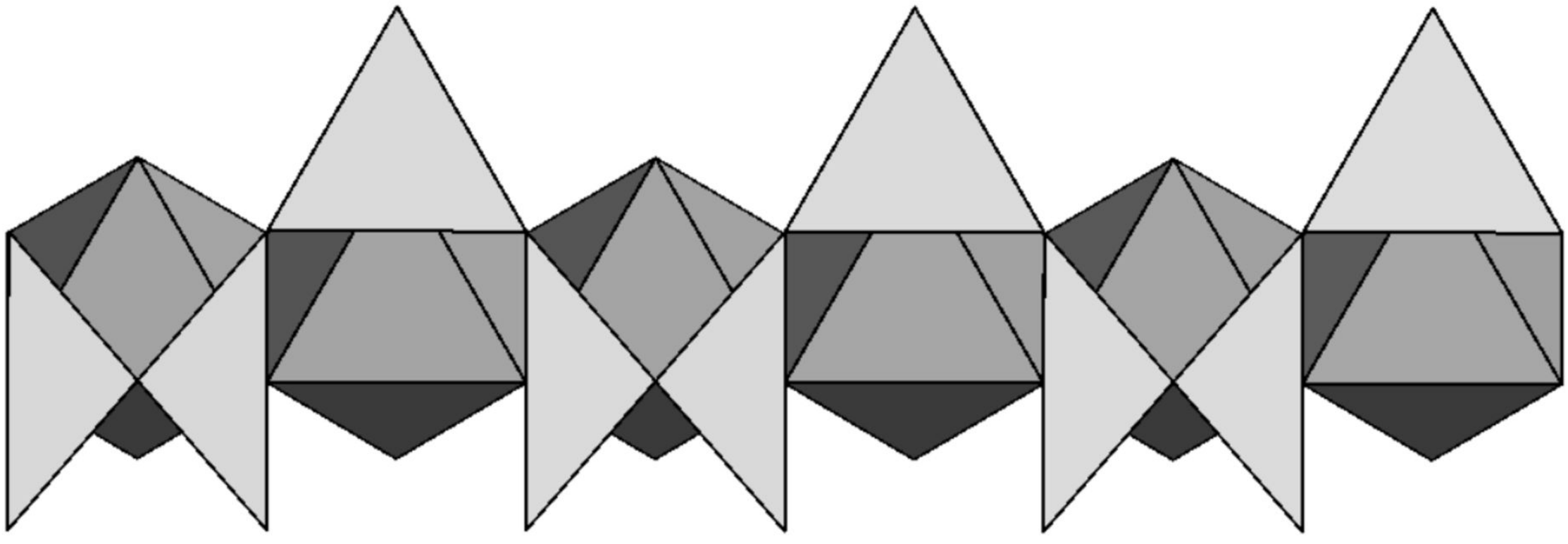

Ideal Wollastonite-1A

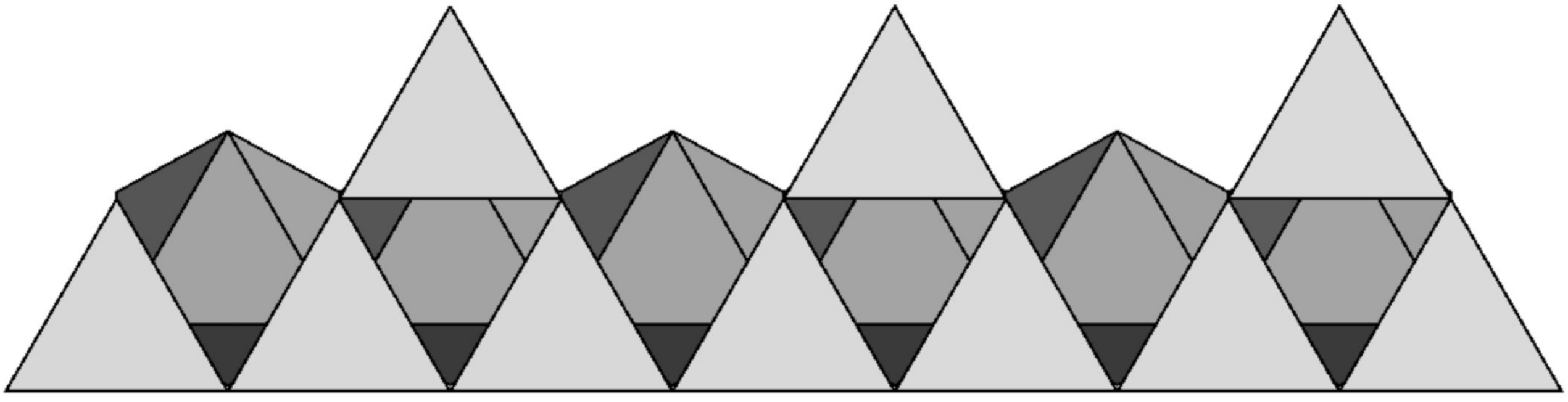

Closest-Packing

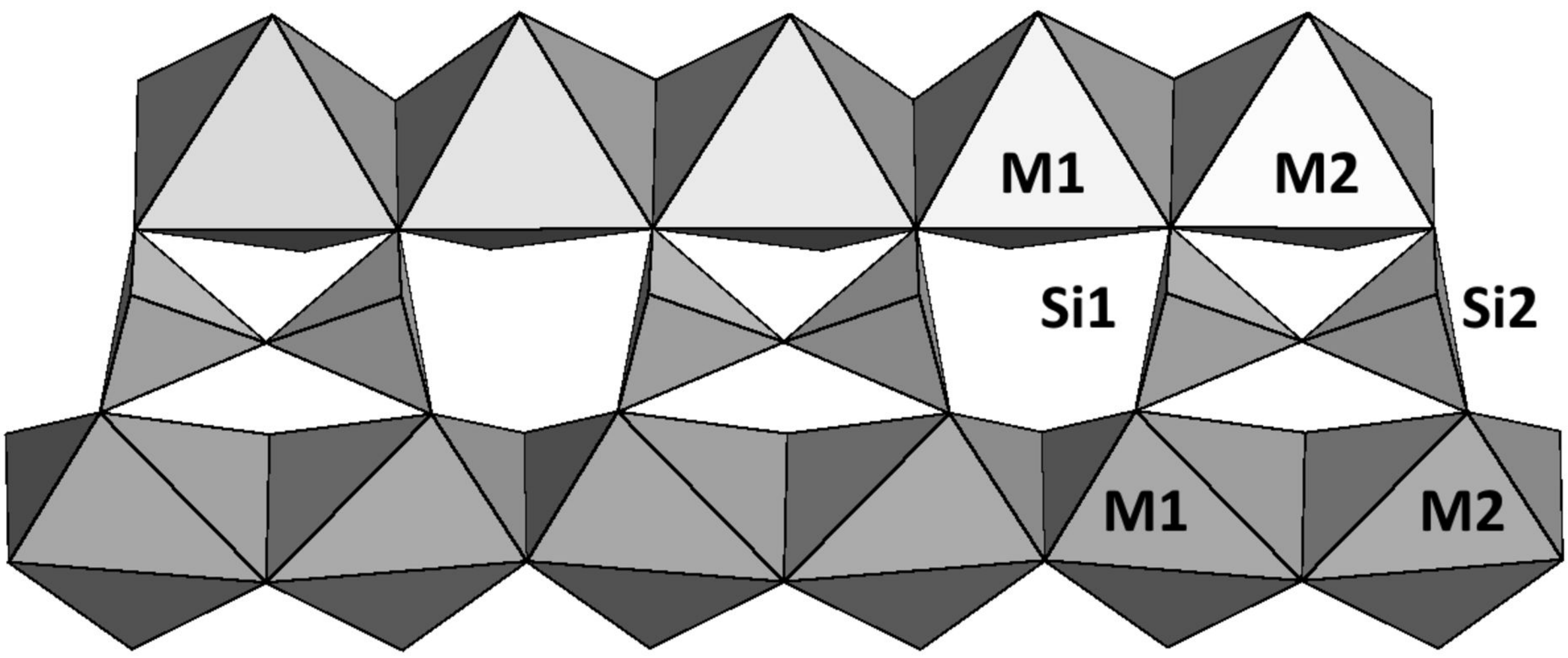

Observed Wollastonite-1A

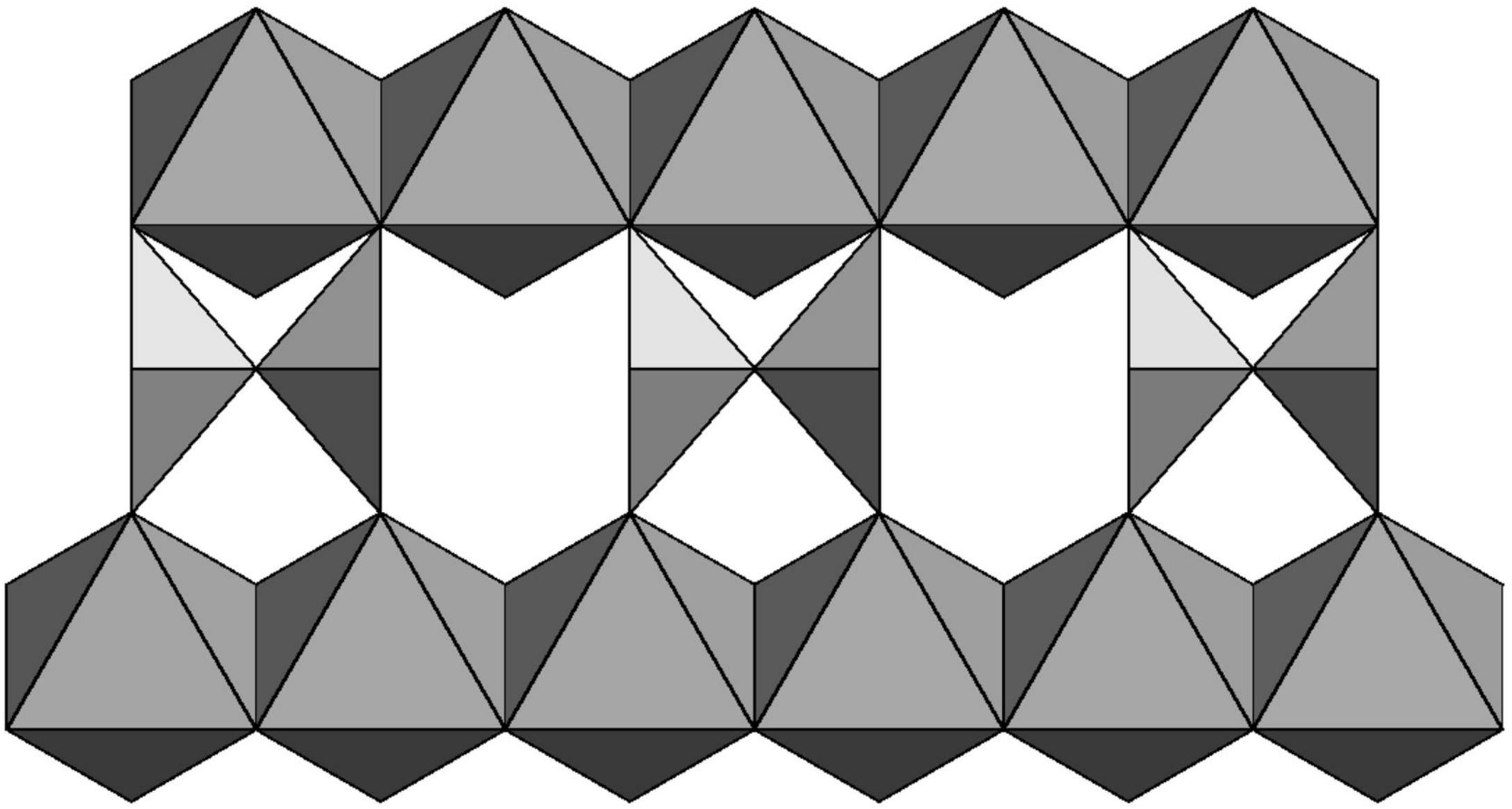

Ideal Wollastonite-1A

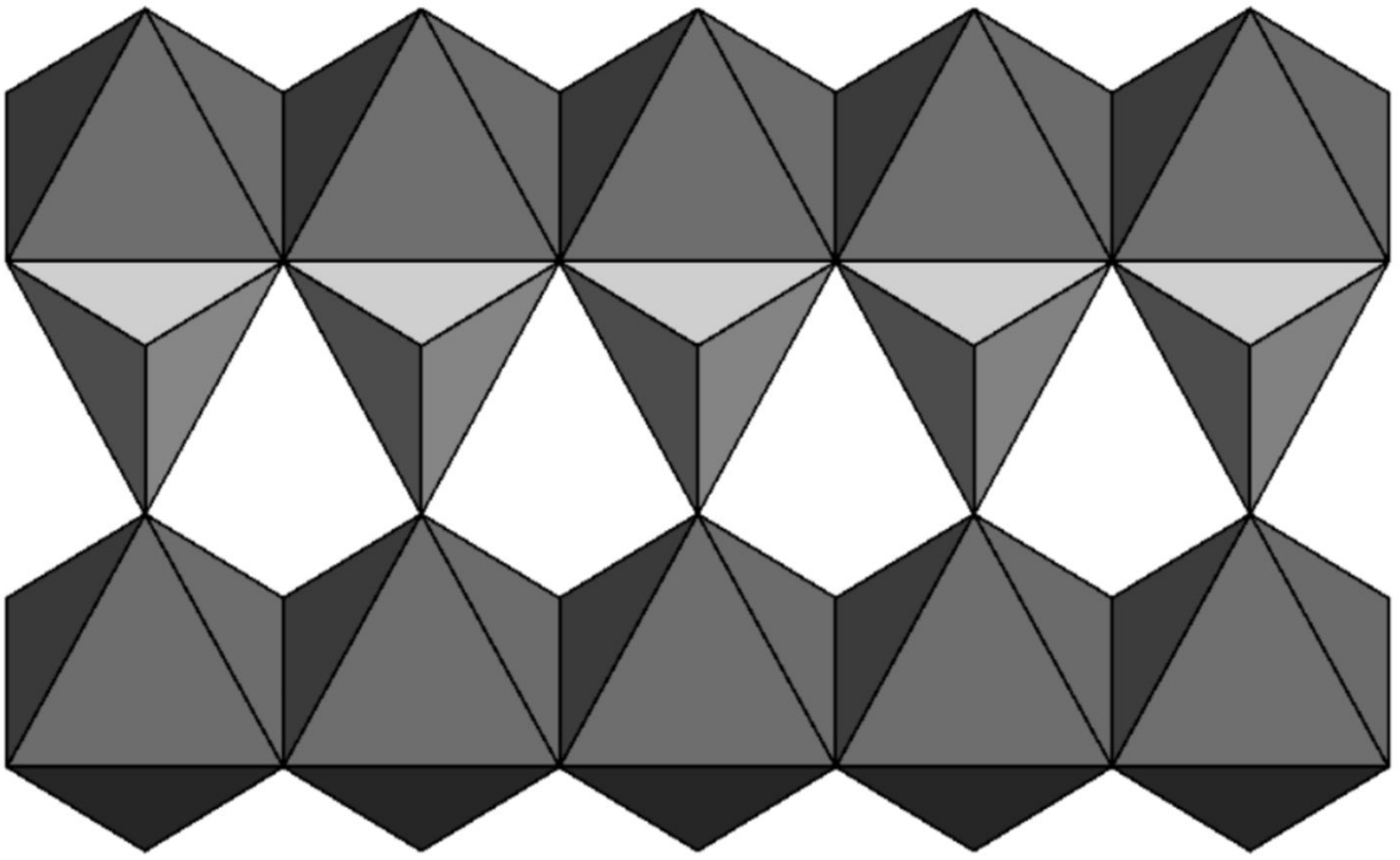

Closest-Packing

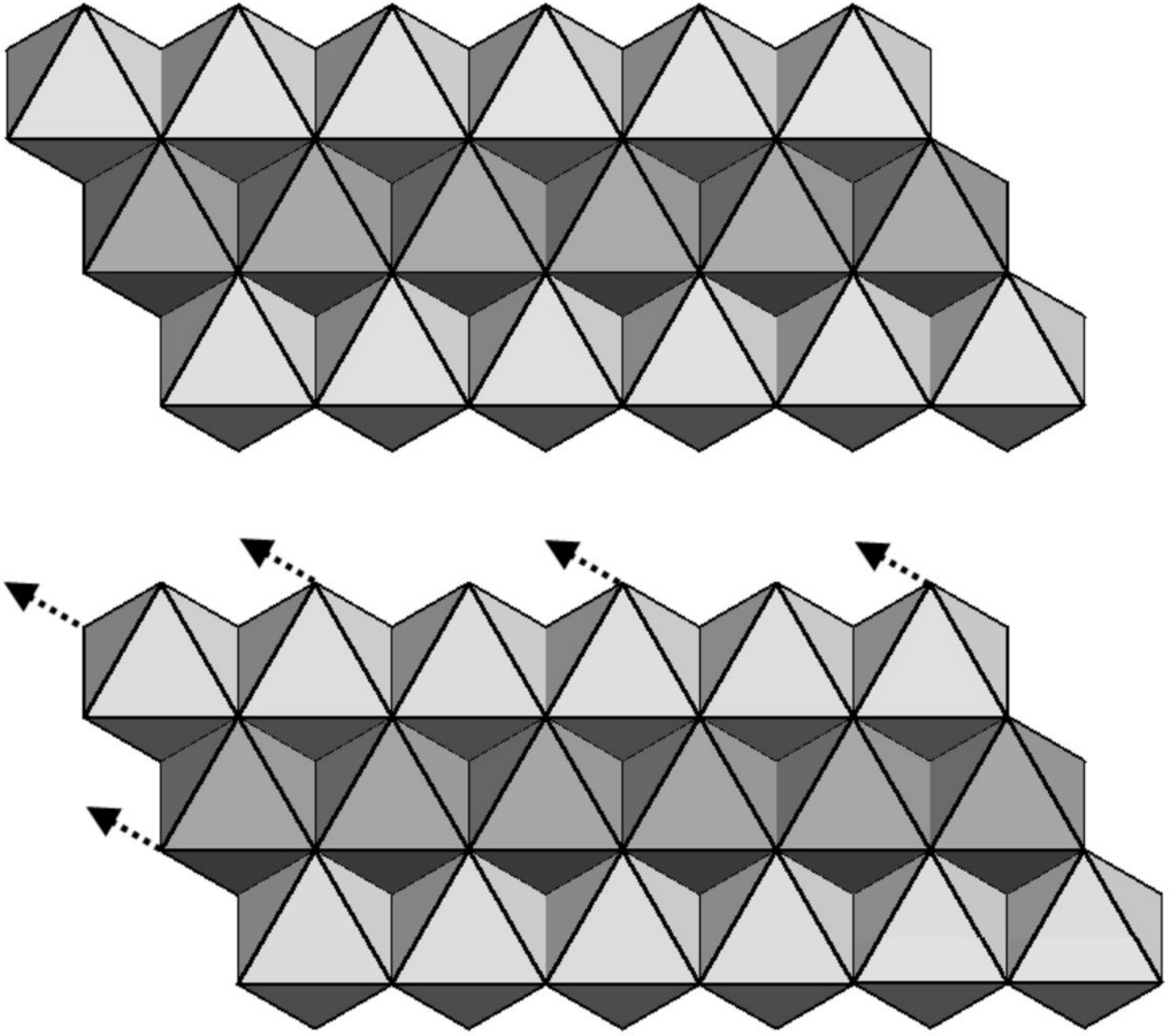

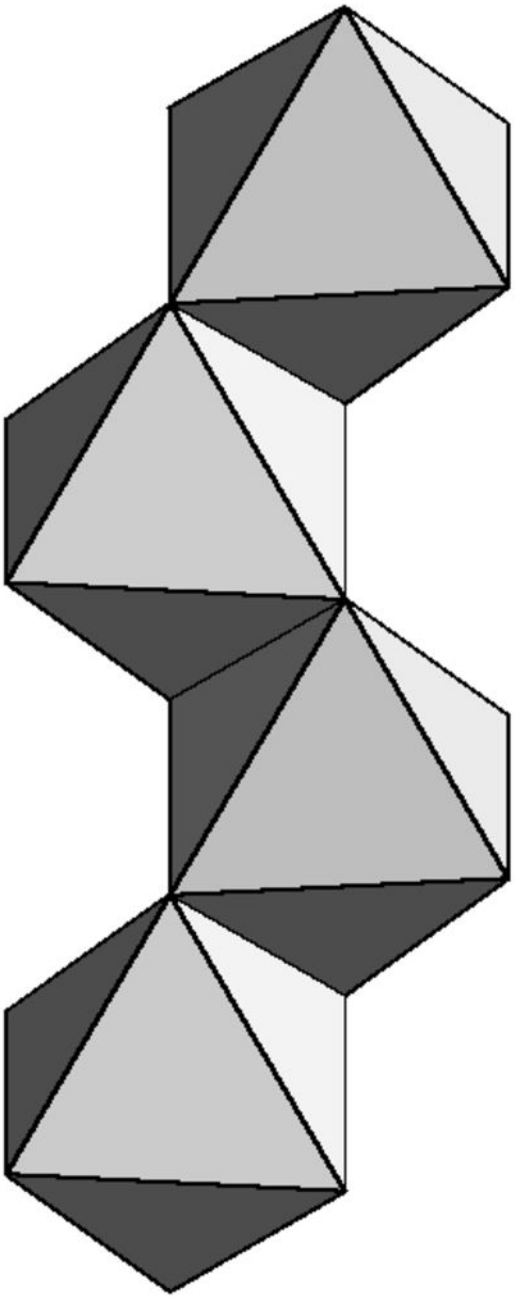

Observed
Diopside

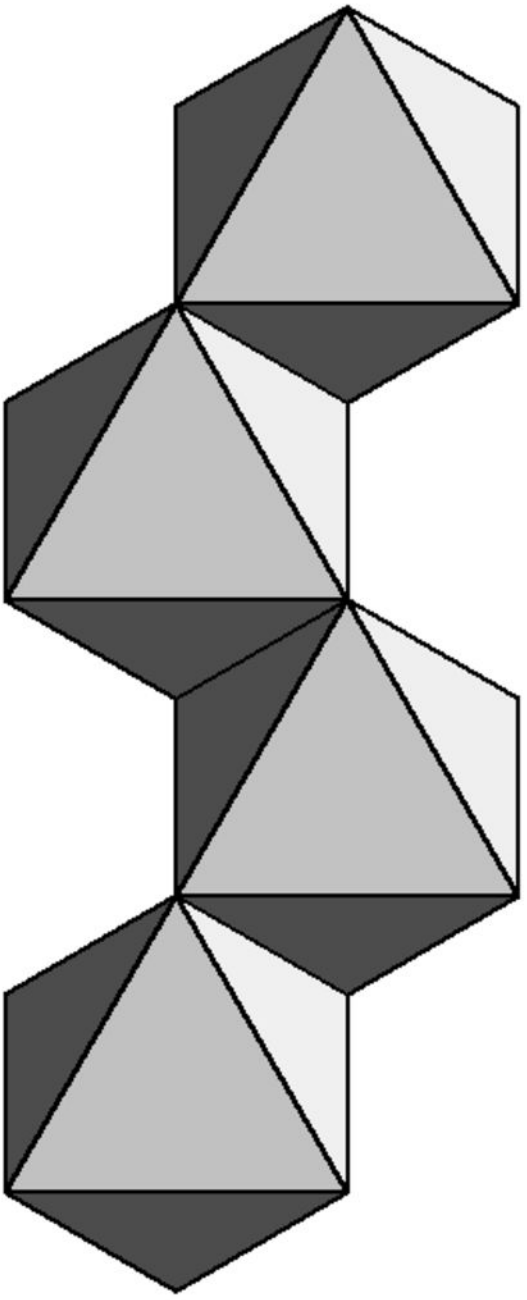

Ideal
Diopside

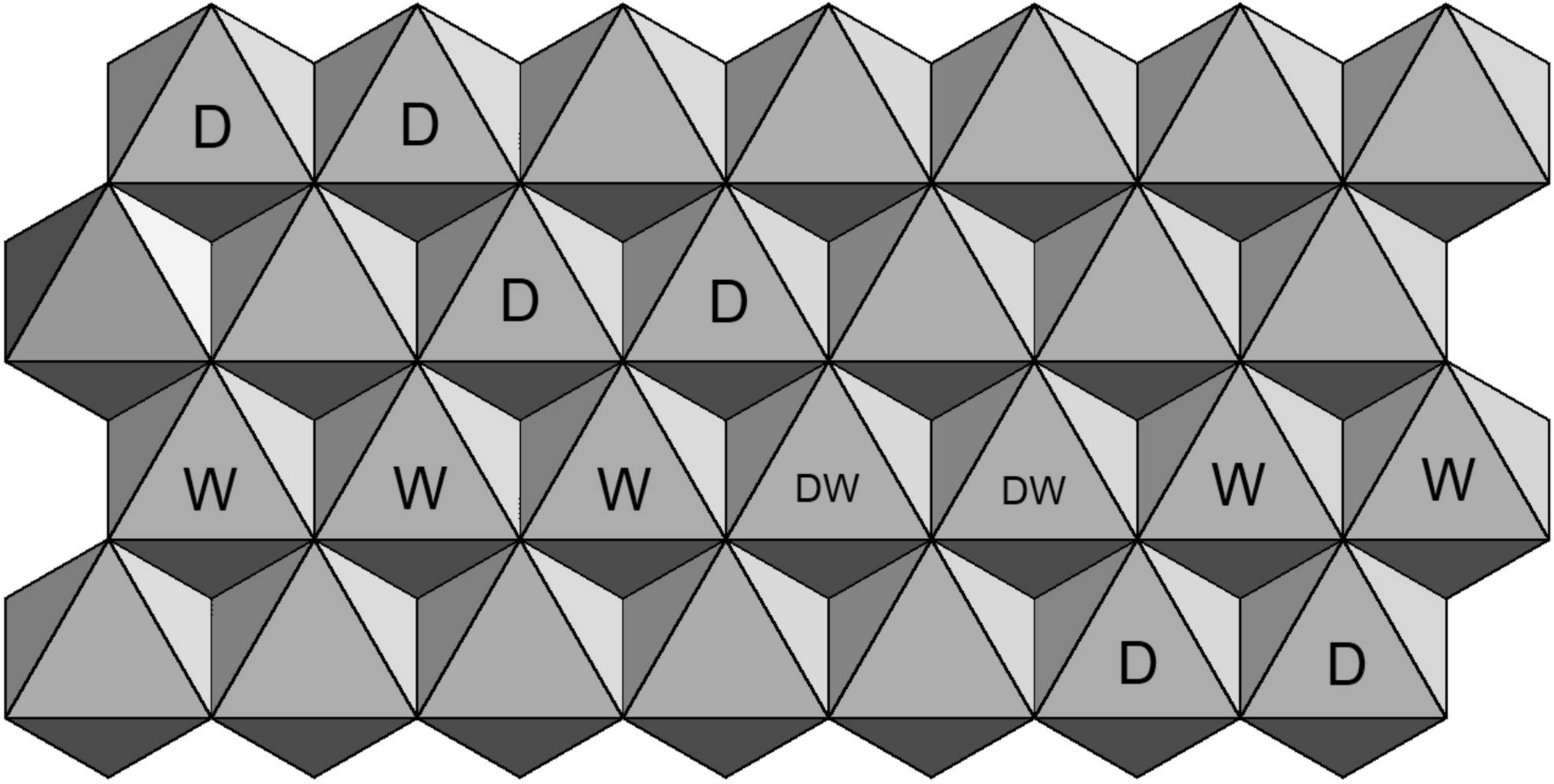
D
D
D
D
W
W
W
DW
DW
W
W
D
D

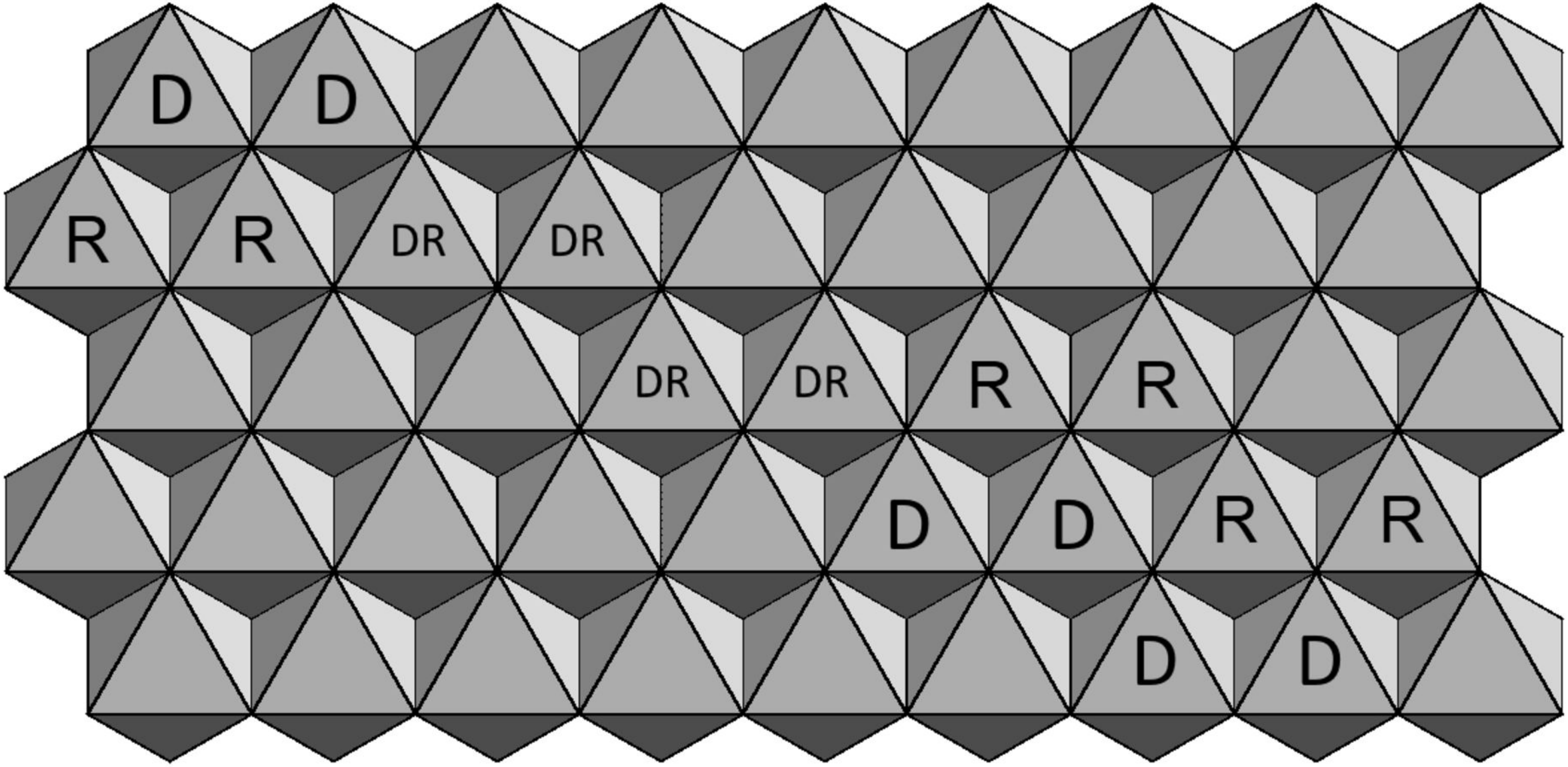
D
D
R
R
DR
DR
DR
DR
R
R
D
D
R
R
D
D

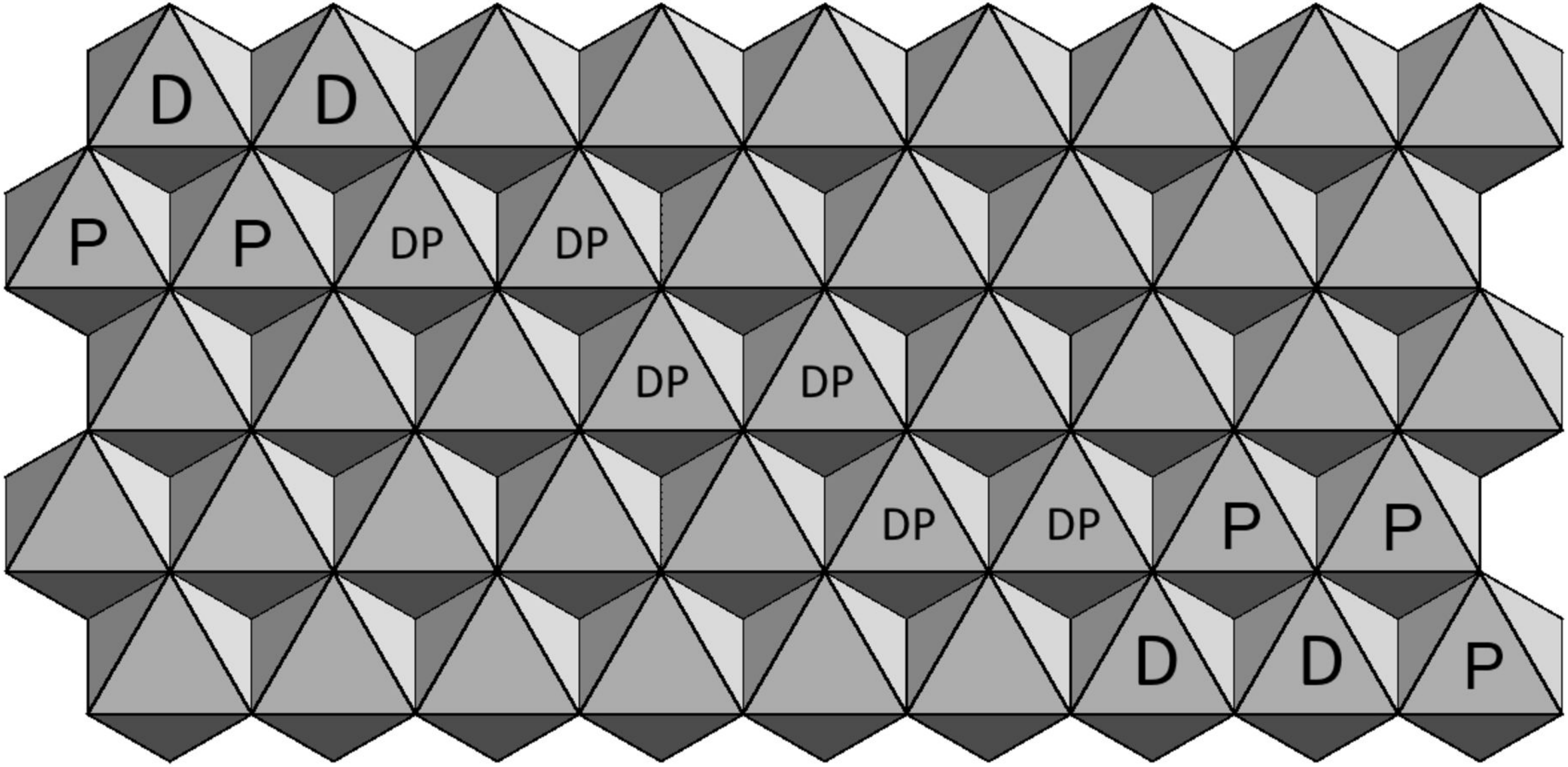
D
D
P
P
DP
DP
DP
DP
DP
DP
P
P
D
D
P

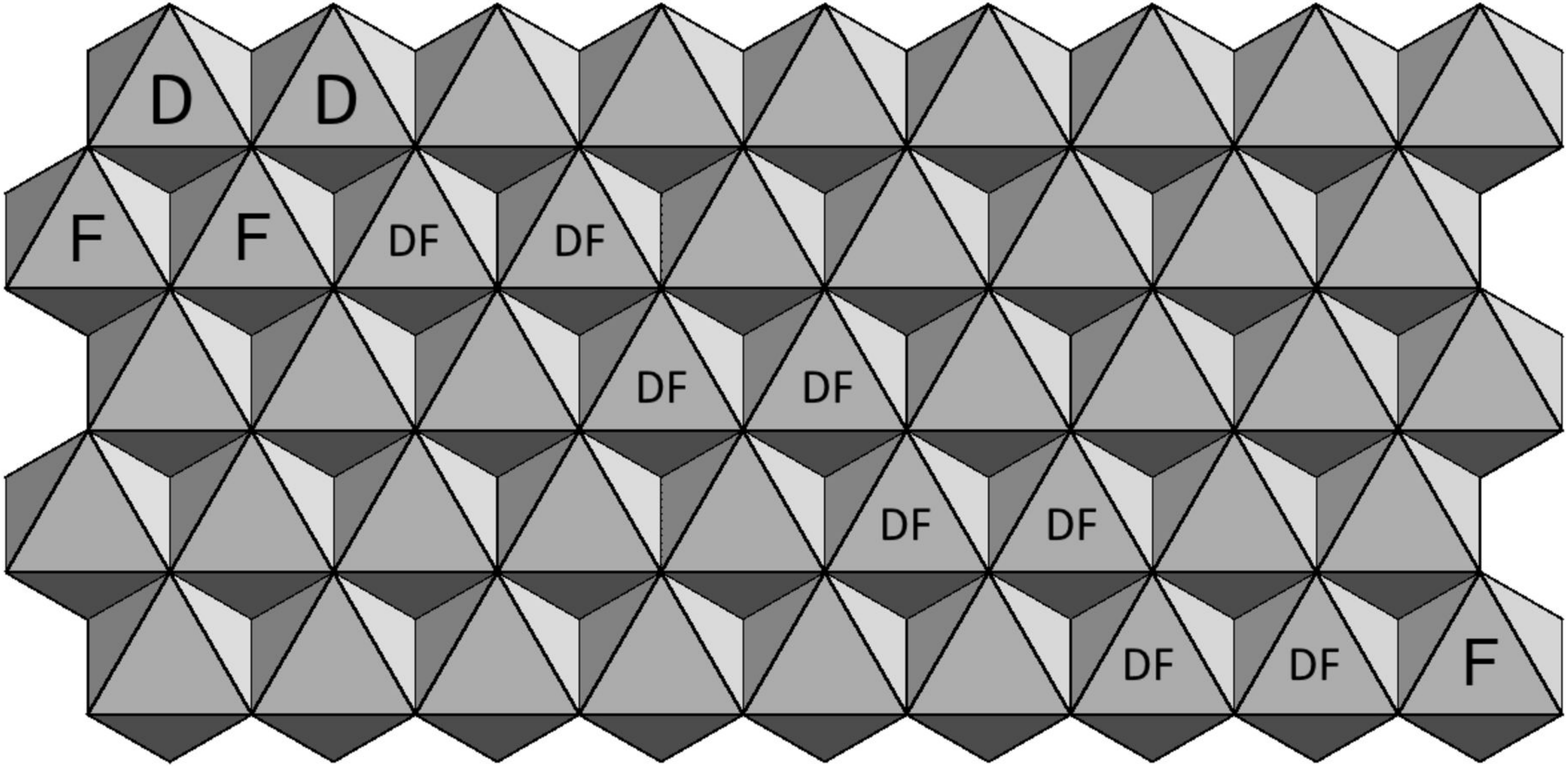
D
D
F
F
DF
DF
DF
DF
DF
DF
DF
DF
F

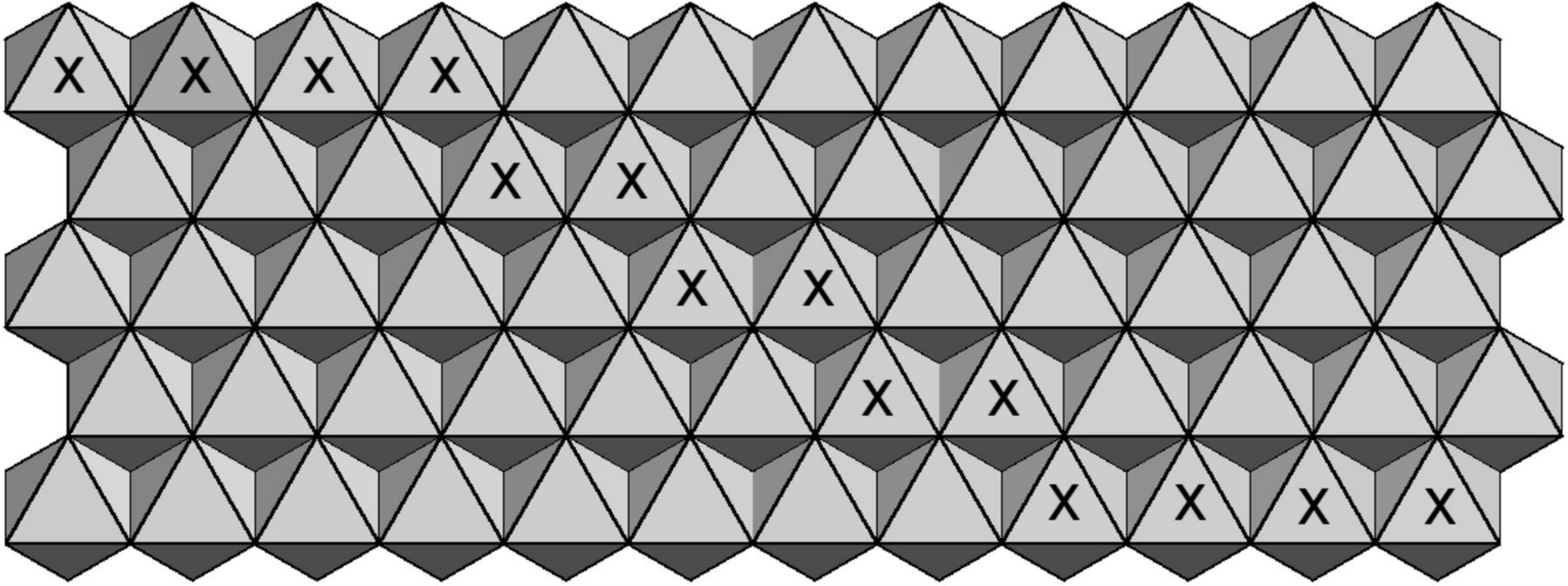
X
X
X
X
X
X
X
X
X
X
X
X
X
X
X
X

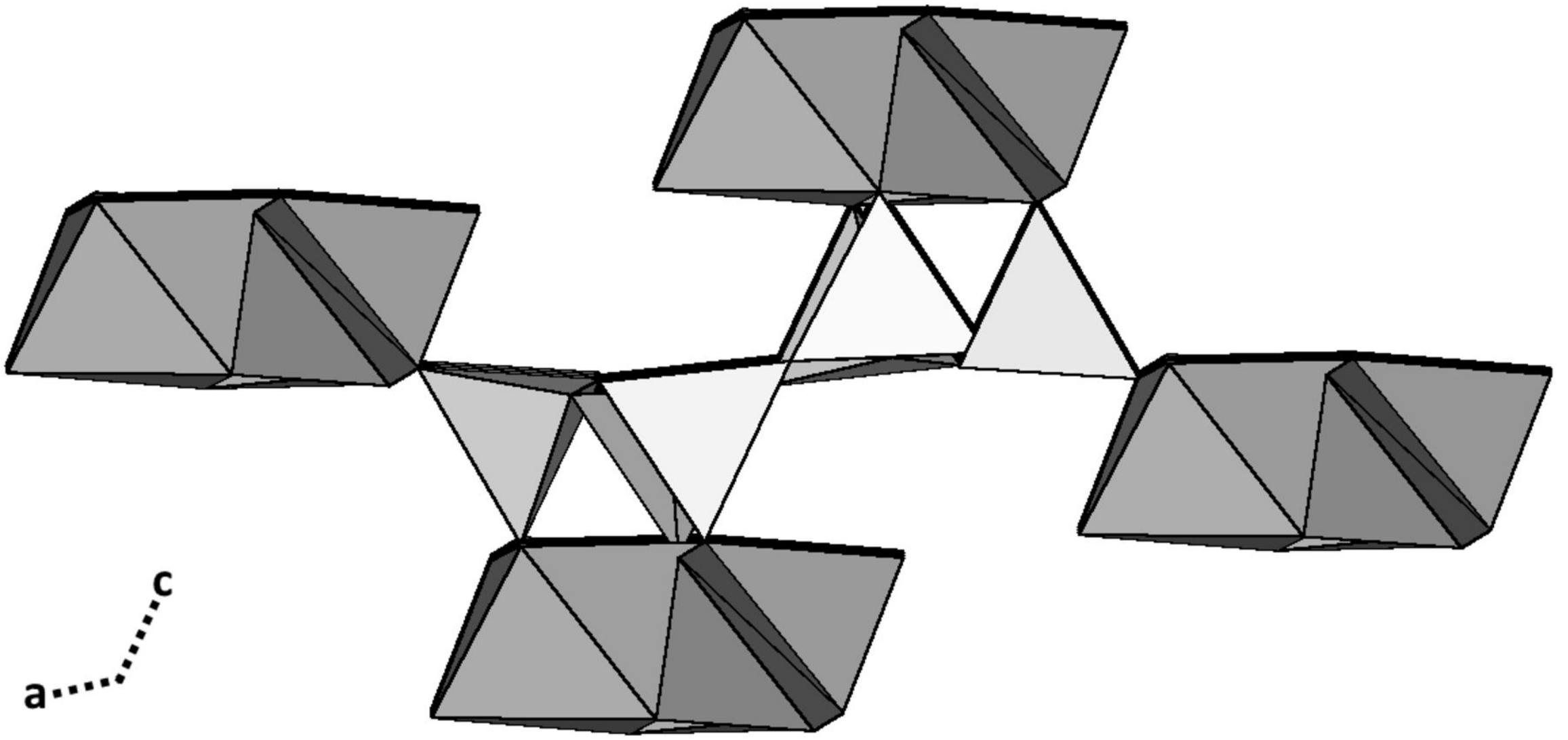

Yangite

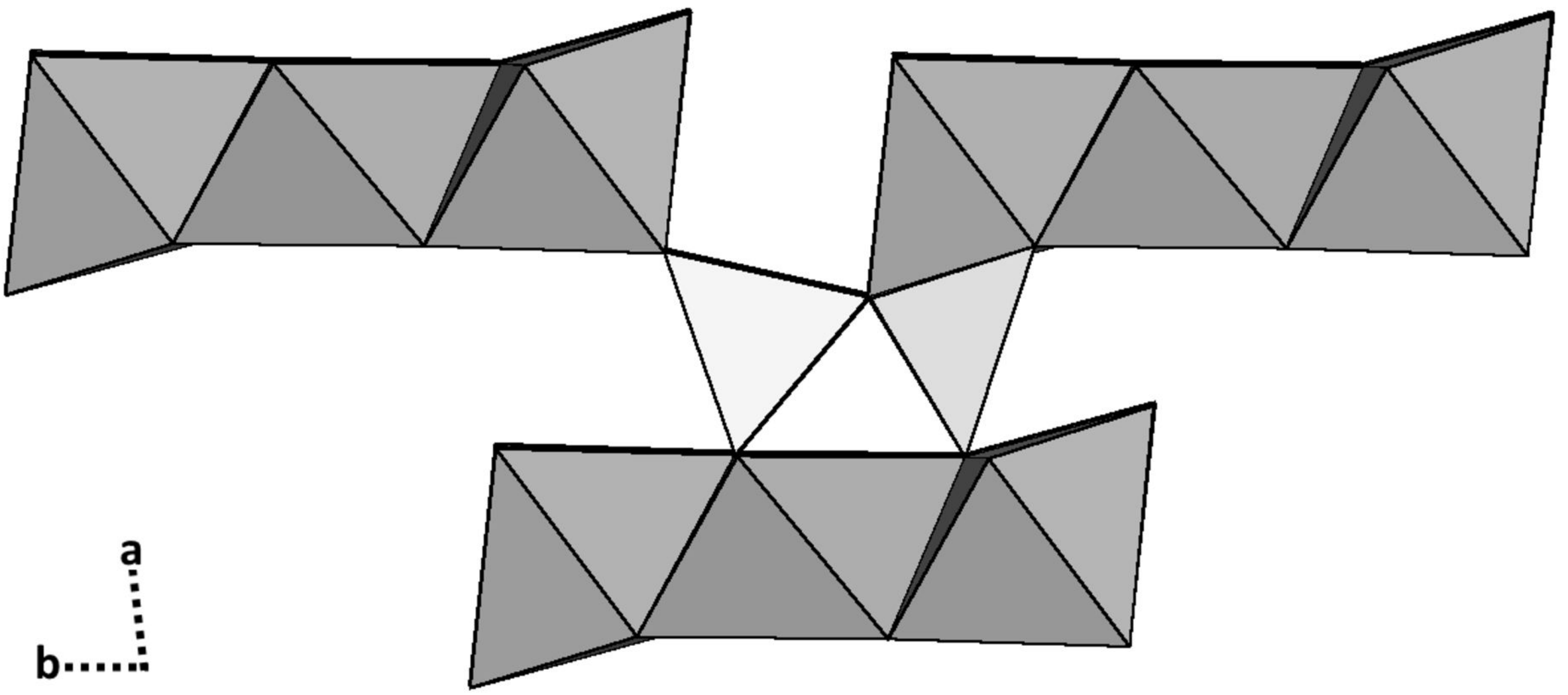

Wollastonite

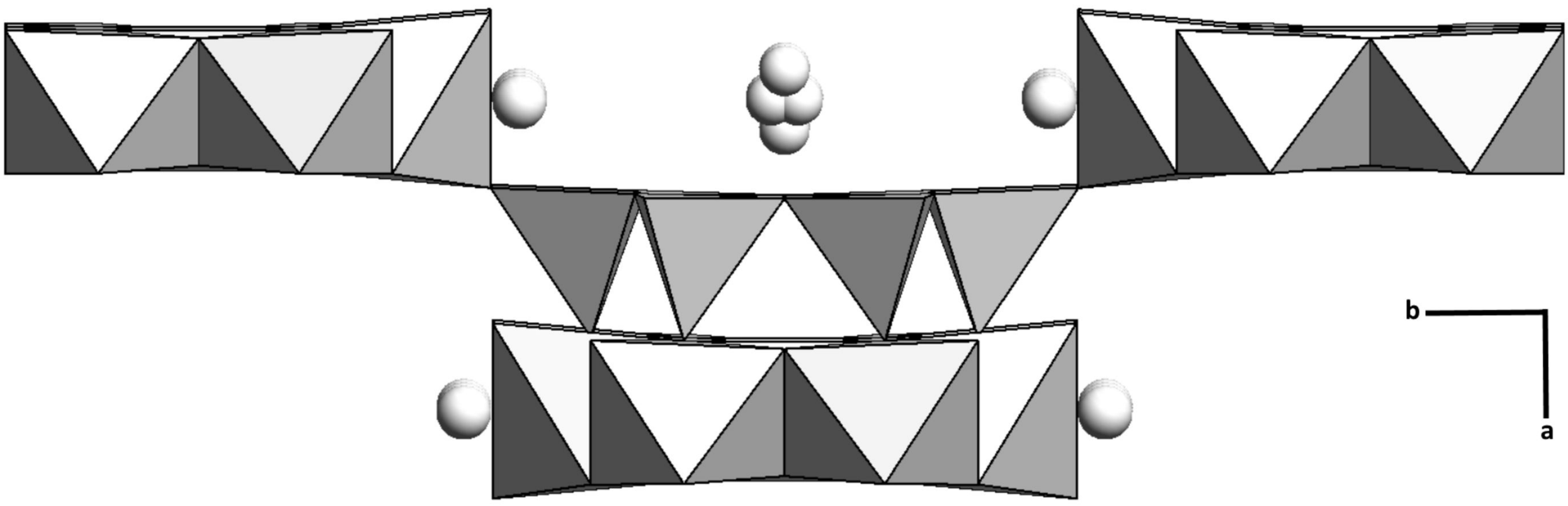

Obertiite

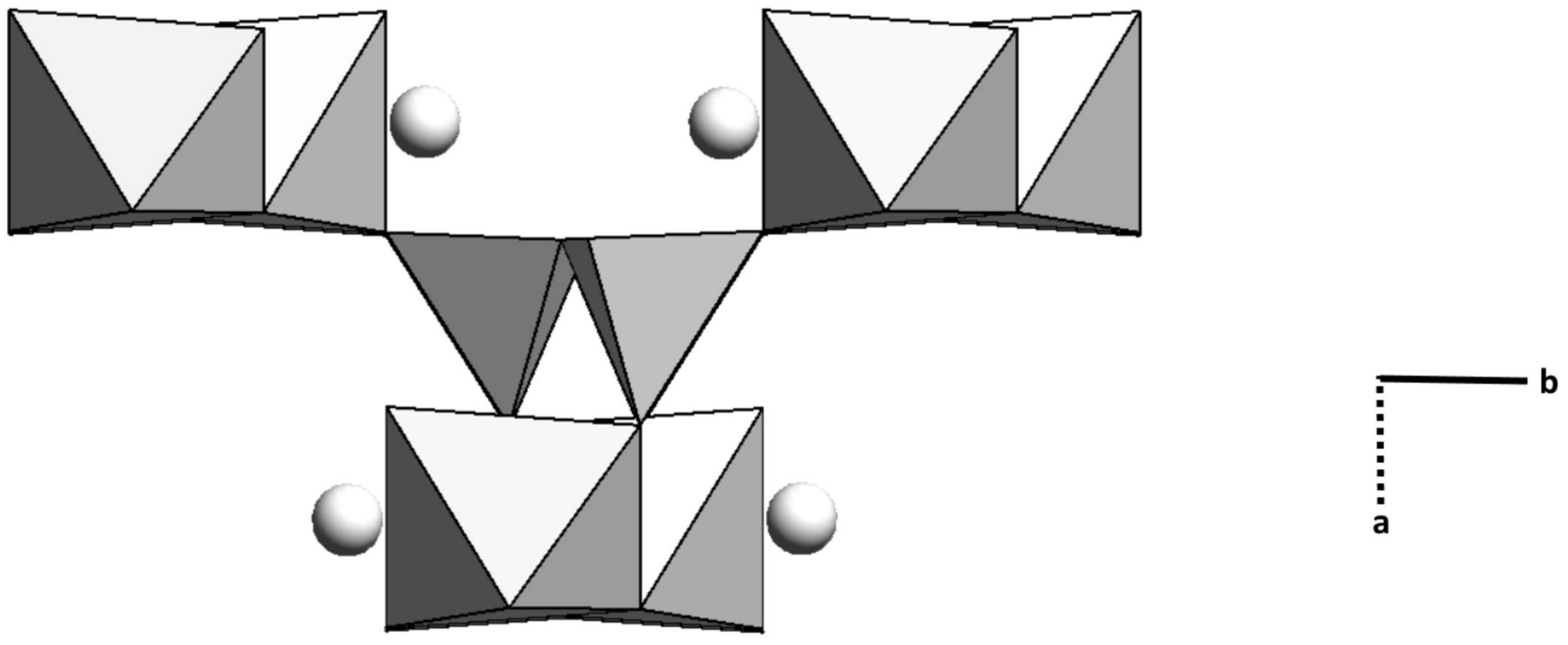

Diopside

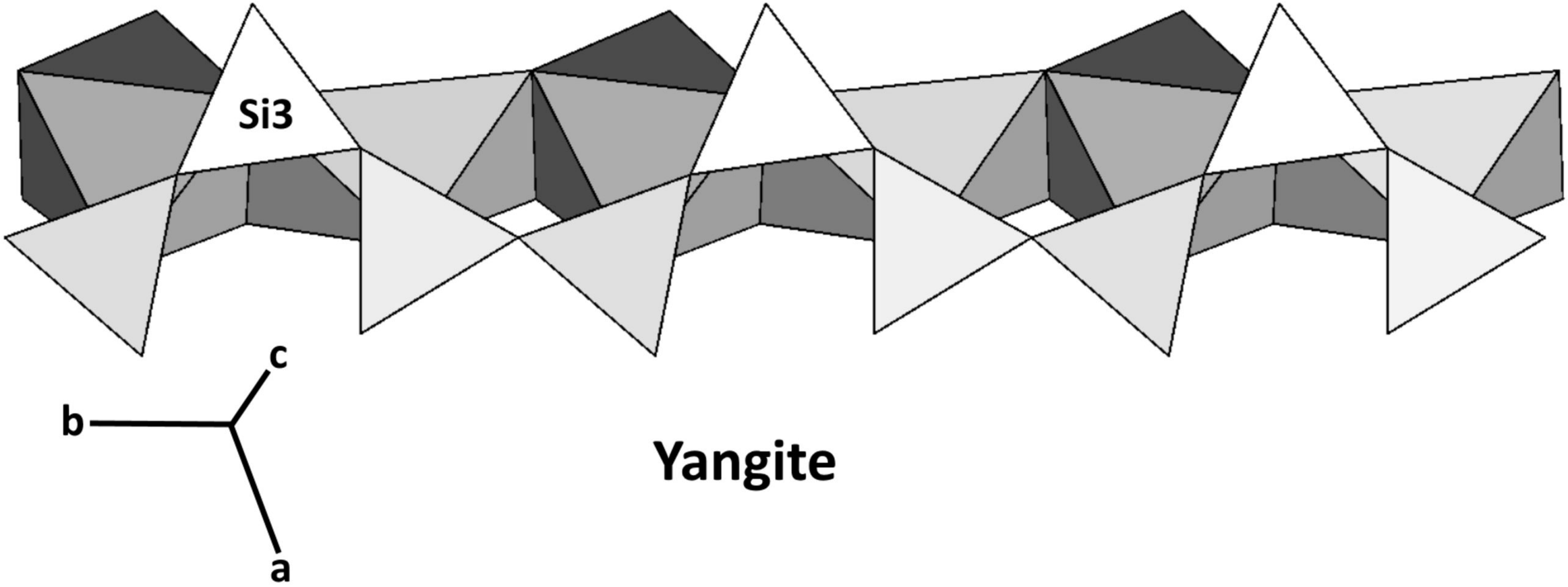

Yangite

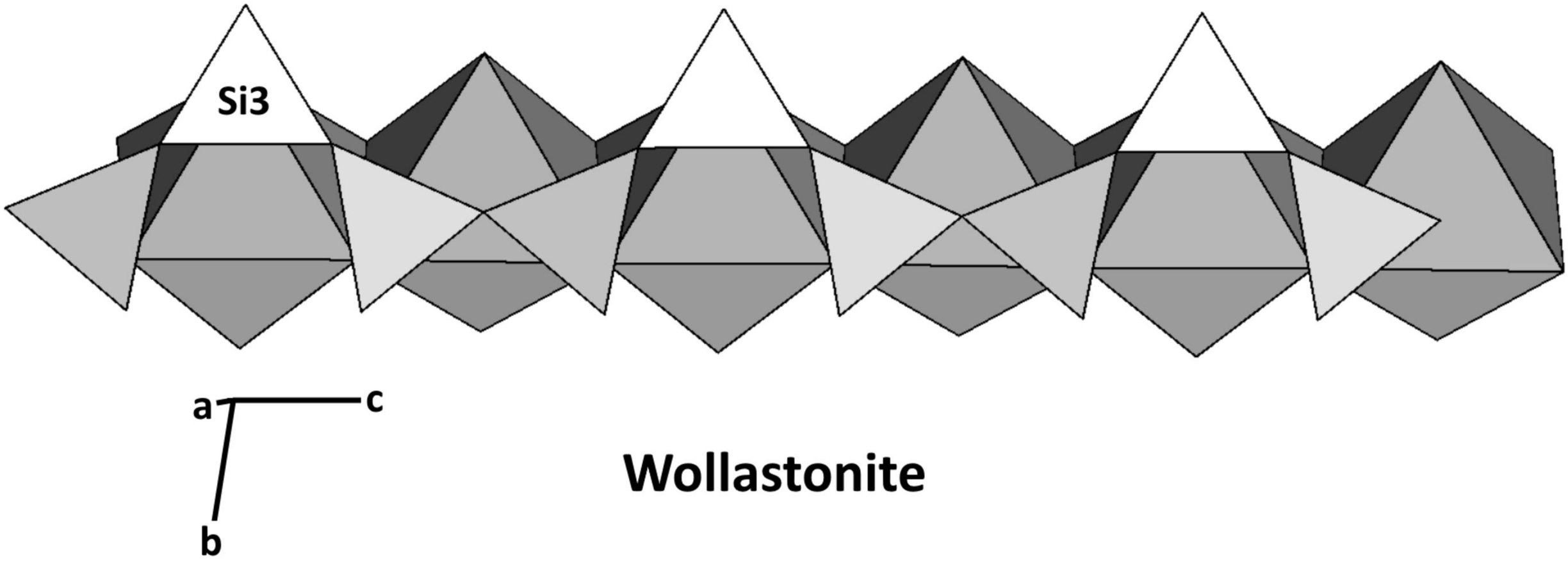

Wollastonite

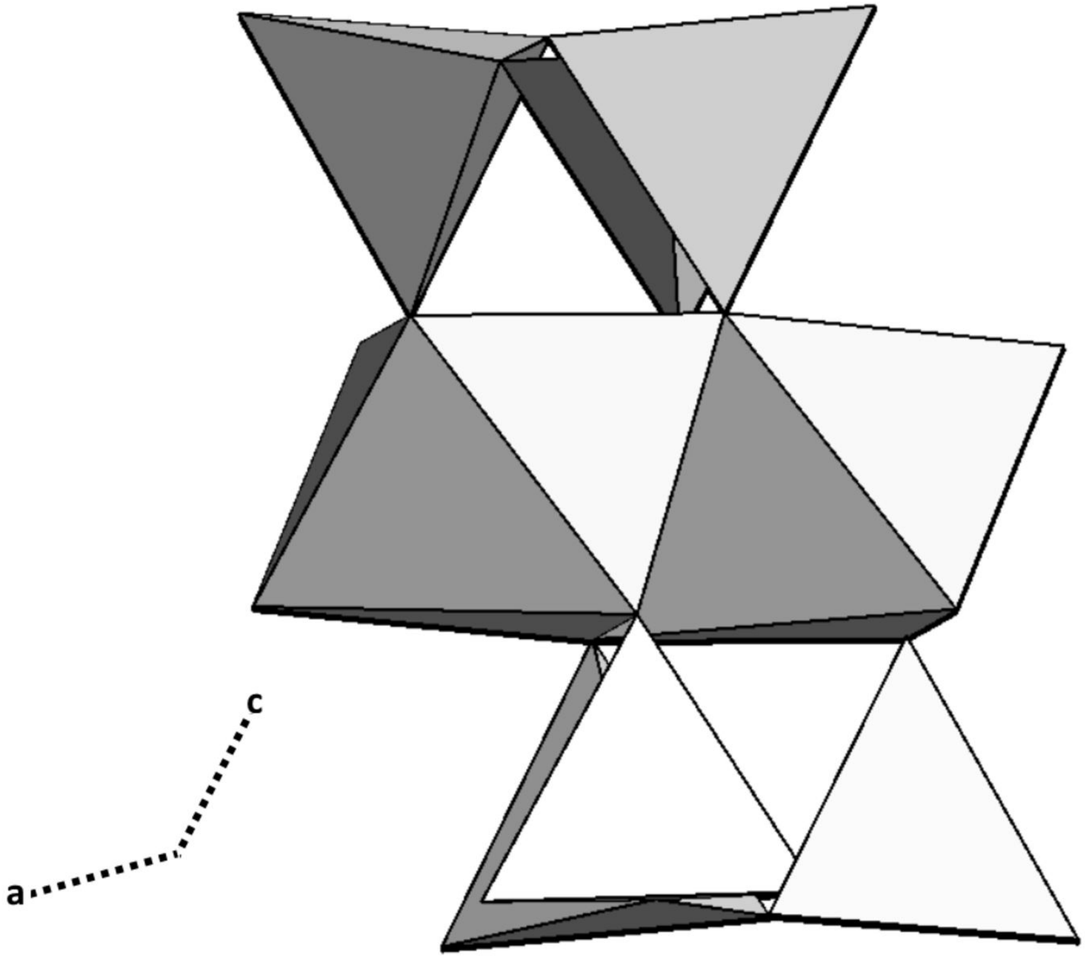

Yangite

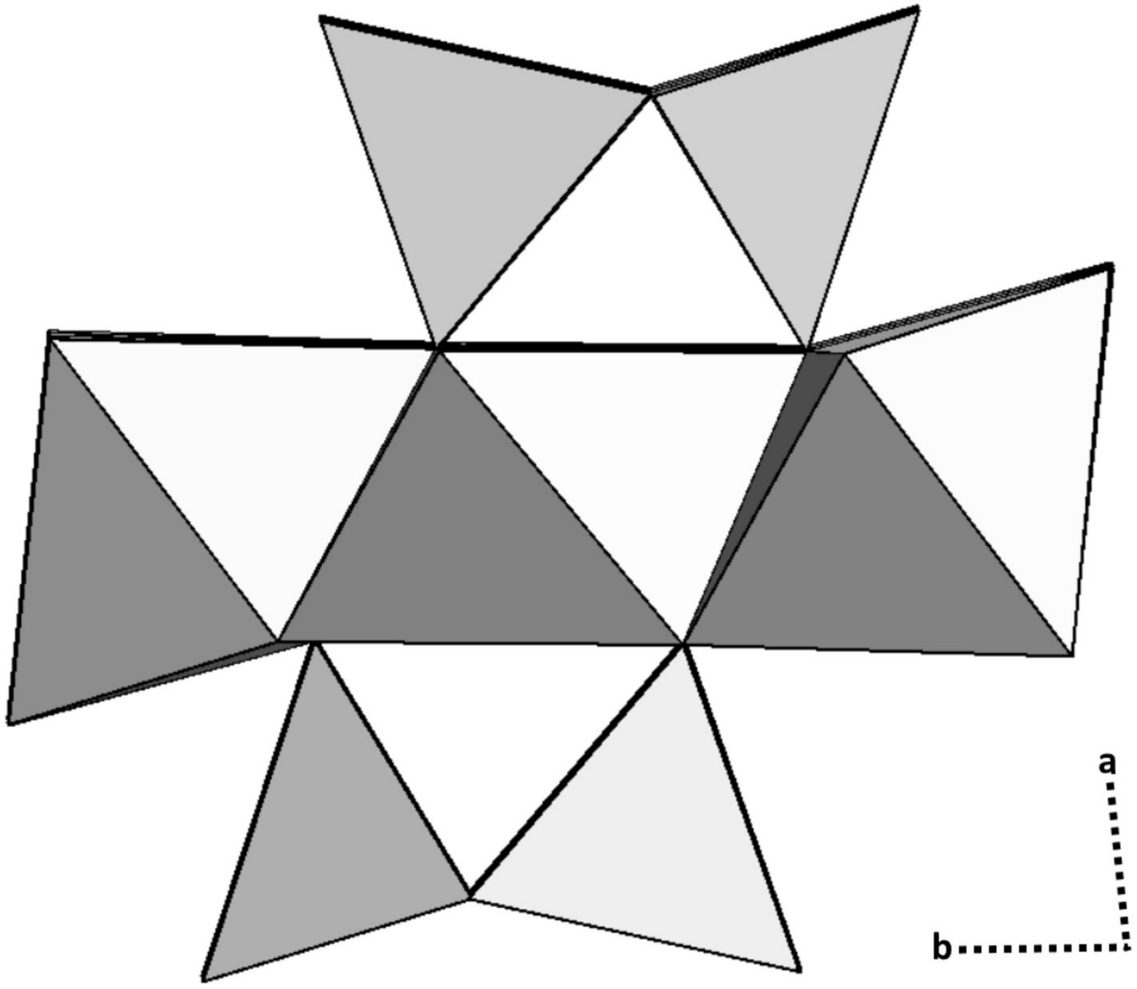

Wollastonite-1A

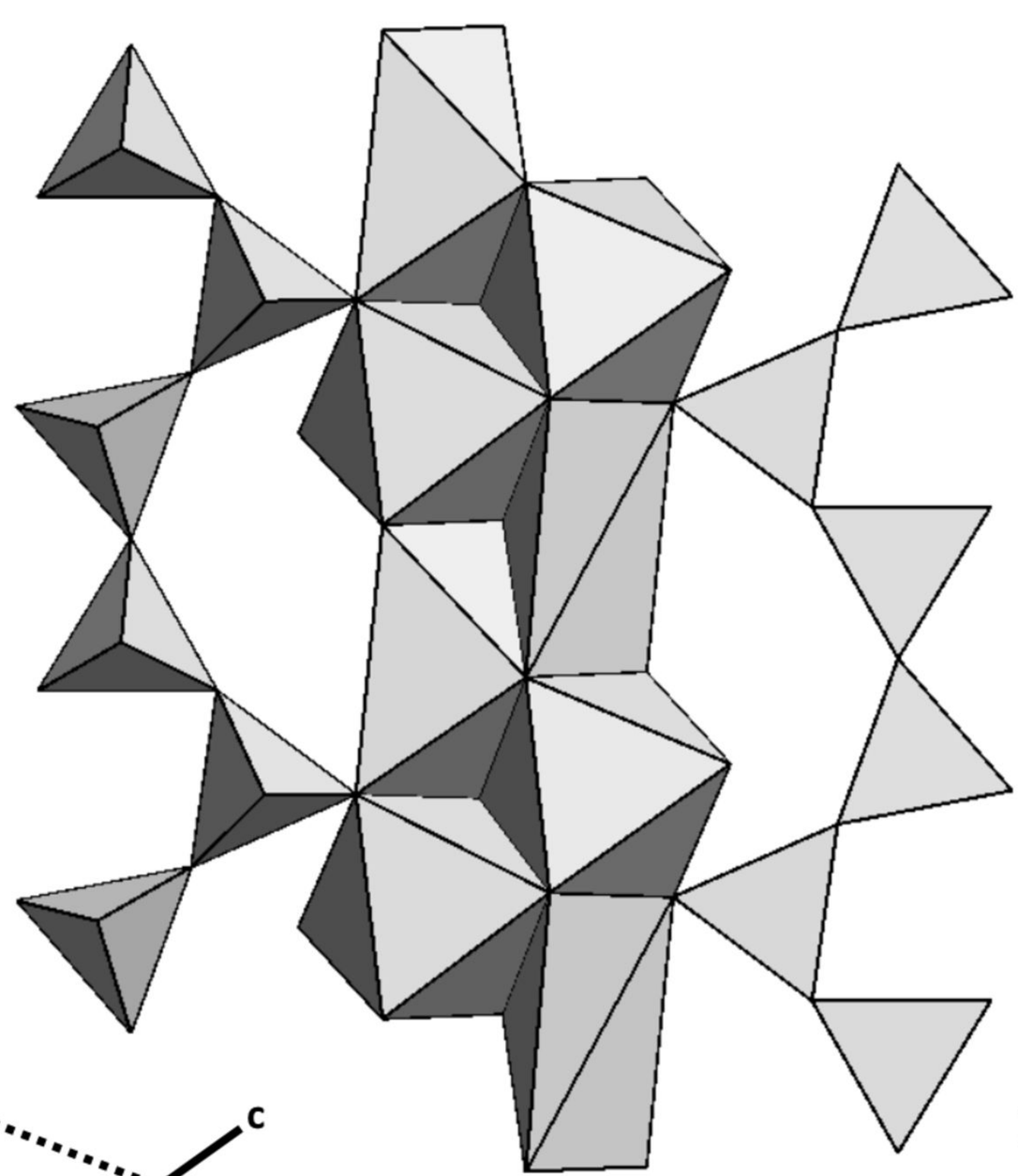

Yangite

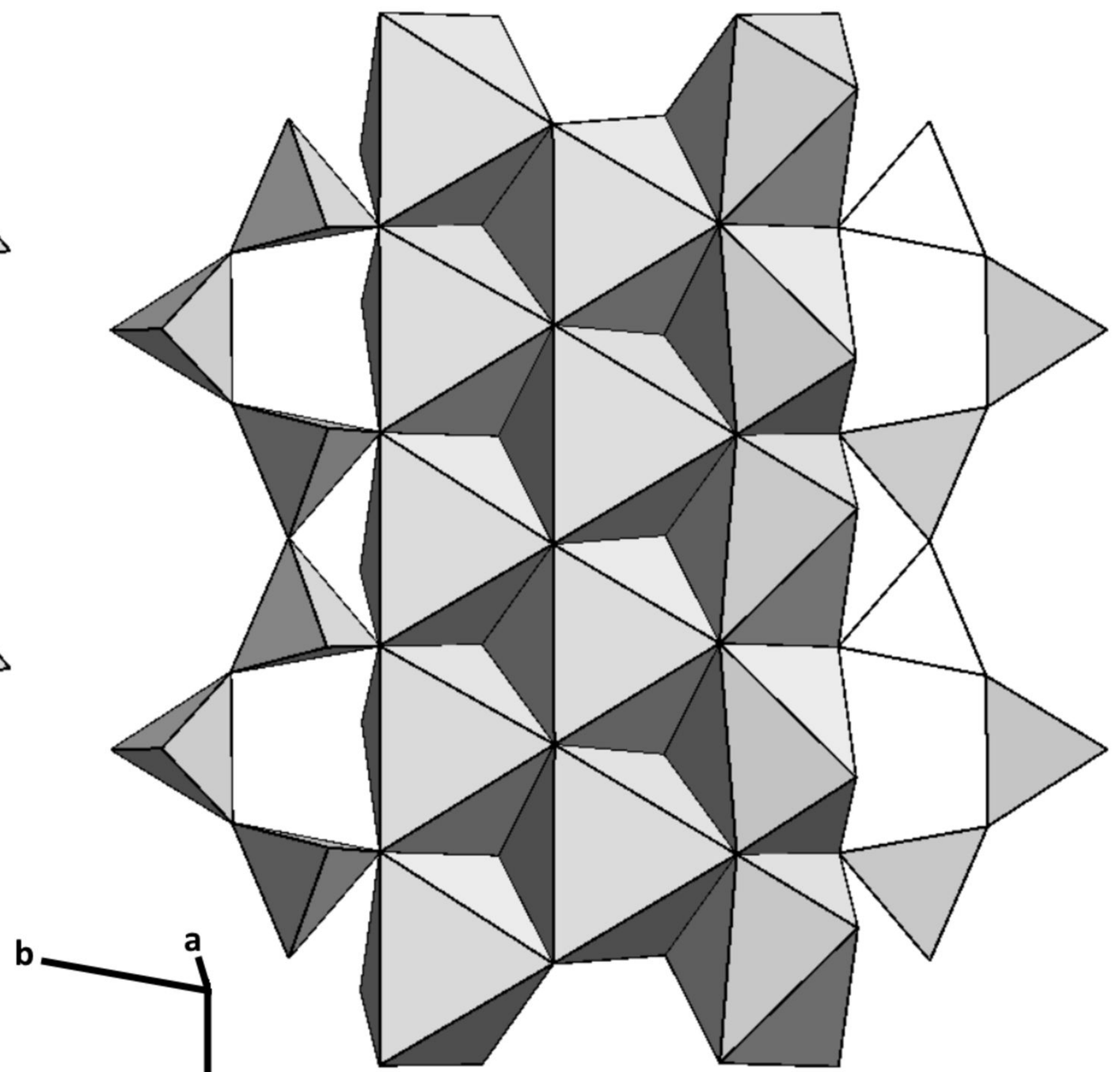

Wollastonite-1A

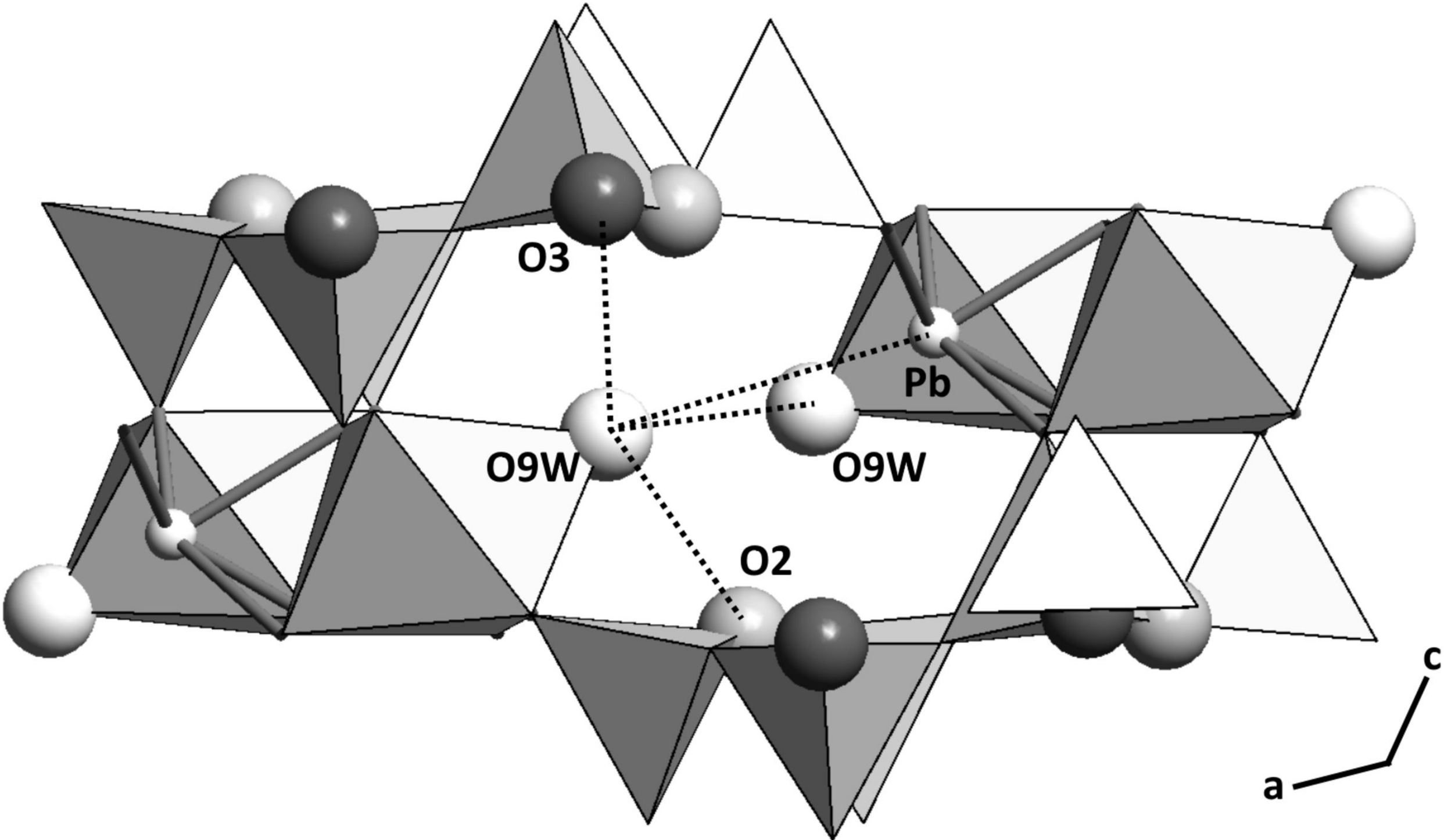
O3
Pb
O9W
O9W
O2
c
a